Beta decays of ^{18}Ne and ^{19}Ne and their relation to parity mixing in ^{18}F and ^{19}F

E. G. Adelberger, M. M. Hindi, C. D. Hoyle,* H. E. Swanson, and R. D. Von Lintig†
Nuclear Physics Laboratory GL-10, University of Washington, Seattle, Washington 98195

W. C. Haxton‡
Theoretical Division, Los Alamos National Laboratory, Los Alamos, New Mexico 87545
and Physics Department, Purdue University, West Lafayette, Indiana 47907
(Received 22 February 1983)

We have studied transitions weakly fed in the β^+ decays of ^{18}Ne and ^{19}Ne. The ^{18}Ne activity was produced by bombarding natural O_2 gas with 12.0 MeV ^{3}He ions. γ-ray groups with energies of 659, 1042, 1081, and 1700 keV were observed with relative intensities of 1.72 ± 0.05, 100.0, $(2.89\pm0.26)\times10^{-2}$, and 0.687 ± 0.013, respectively. These intensities correspond to relative branching ratios of 100.0, $(2.70\pm0.36)\times10^{-2}$, and 2.45 ± 0.05 for β^+ transitions to the 1042, 1081, and 1700 keV levels, respectively. Normalizing to previous data we obtain ft values of 1247 ± 11, 2971 ± 87, $(1.03\pm0.14)\times10^7$, and $(3.00\pm0.10)\times10^4$ sec for the transitions to the ground state, 1042, 1081, and 1700 keV levels, respectively. The difference in excitation energies of the 0^- and 0^+ states is found to be 39.20 ± 0.11 keV. The ^{19}Ne activity was produced by bombarding SF_6 gas by 6.4 MeV protons. A branching ratio of $(1.20\pm0.20)\times10^{-4}$ was obtained for the transition to the 110 keV level which corresponds to an ft value of $(1.15\pm0.19)\times10^7$ sec. Transitions to the 1554 keV level were observed in a 9.2% Ge(Li) detector operated in the singles mode. A branching ratio of $(2.34\pm0.30)\times10^{-5}$ was obtained which corresponds to an ft value of $(5.01\pm0.47)\times10^5$ sec. The ^{18}Ne$(0^+;1)\rightarrow{}^{18}$F(1081 keV $0^-;0$) and ^{19}Ne$(\frac{1}{2}^+;\frac{1}{2})\rightarrow{}^{19}$F (110 keV $\frac{1}{2}^-;\frac{1}{2}$) first-forbidden β^+ branches are analogs of the previously measured parity mixing of the 1042 keV $(0^+;1)$ and 1081 $(0^-;1)$ keV levels of ^{18}F and of the ground $(\frac{1}{2}^+;\frac{1}{2})$ and 110 keV $(\frac{1}{2}^-;\frac{1}{2})$ levels of ^{19}F, respectively. We show that the strong exchange-current corrections to the axial charge operator dominating these β transitions involve an operator identical, apart from an isospin rotation, to that mediating the pion-exchange contribution to the parity nonconserving NN force. These exchange current contributions can be extracted from the β-decay rates in a manner nearly independent of nuclear structure assumptions. Thus, in these cases, the usual structure uncertainties that obscure the connection between the $\Delta S=0$ weak hadronic interaction and nuclear observables can largely be circumvented. The ft values we obtain for the transitions to the 1081 keV and 110 keV levels of ^{18}F and ^{19}F suggest that the strengths of the $I=1$ and $I=0$ components of the parity nonconserving NN force are close to the "best values" of Desplanques, Donoghue, and Holstein. Except for a recent structure calculation employing complete $2h\omega$ and $1h\omega$ bases for the positive and negative parity states in ^{18}F, the β decay and parity nonconserving matrix elements predicted in typical shell model studies are approximately three times larger than experiment. This and other evidence suggests that the softening of the nuclear Fermi surface by $2h\omega$ configurations is an essential, but missing, feature of most nuclear structure calculations of parity nonconserving matrix elements. We conclude by presenting shell model studies of the electromagnetic properties of low-lying states in ^{18}F, ^{19}F/^{19}Ne, and ^{21}Ne/^{21}Na as well as the matrix elements for the operators that arise in a general meson-exchange parity nonconserving potential.

[RADIOACTIVITY ^{18}Ne, ^{19}Ne; measured $I\gamma$; deduced ft. Compared to shell model calculations. Discussed connection of forbidden decays to parity mixing in ^{18}F and ^{19}F.]

I. INTRODUCTION

At low energies the parity-nonconserving (PNC) NN force can be characterized by the amplitudes for five elementary S-P transitions: $^1S_0$-$^3P_0$, $\Delta I=0,1,2$, $^3S_1$-$^1P_1$, $\Delta I=0$, and $^3S_1$-$^3P_1$, $\Delta I=1$. One can, in principle, infer six amplitudes from low energy experiments since the $\pi^{\pm}$ exchange contribution to the $^3S_1$-$^3P_1$ amplitude can be separated from the shorter range contributions of the heavier mesons. It is an interesting and important challenge to our understanding of hadronic weak processes to measure all six of these amplitudes and compare them to theoretical predictions derived from the meson exchange mechanism in which one of the vertices is governed by the strong interaction and the other by the weak.

In the best of all possible worlds one would have at least six PNC experiments in the NN system, each of which measured a different combination of the six amplitudes. However, the expected effects are very small and the experiments are quite difficult. Experiments sensitive to three different pseudoscalar observables have been reported:

(1) The helicity dependence of the total cross section for $p+p$ scattering has been measured at $E_p=15$ MeV (Ref 1) and $E_p=45$ MeV.[2] These data are sensitive in varying degrees to all three $^1S_0$-$^3P_0$ amplitudes (amplitudes involving $I=0$ states clearly cannot contribute to $p+p$) and are the only definite PNC effects observed in the NN system.

(2) The circular polarization (P_γ) of the 2.2 MeV γ radiation emitted when thermal neutrons are captured by hydrogen has been studied.[3] This observable is sensitive to the $\Delta I=0,2$ $^1S_0\rightarrow{}^3P_0$ and the $\Delta I=0$ $^3S_1\rightarrow{}^1P_1$ amplitudes,[4] but the experimental limit,[3] $P_\gamma\lesssim 5\times10^{-7}$, is greater than the predicted effect.

(3) The asymmetry (A_γ) of the 2.2 MeV radiation emitted when polarized thermal neutrons are captured by hydrogen is sensitive to the $^3S_1\rightarrow{}^3P_1$ $\Delta I=1$ amplitudes,[4] but the experiment[5] has not yet reached the precision needed to measure an effect.

The remaining two-body experiments required to determine all six parameters of the PNC NN force are considerably more difficult than those discussed above. One is therefore led to examine relatively simple examples of PNC in complex nuclei that are practical on experimental grounds and yet tractable theoretically. Particularly promising opportunities exist in certain light nuclei where nearly degenerate doublets of states with the same spin but opposite parity are found at low excitation energy. The most important examples are shown in Fig. 1. In such cases, a PNC observable, such as a net circular polarization or angular asymmetry (for a polarized nucleus) of photons emitted by one state of the doublet, is largely determined by a single PNC nuclear matrix element connecting the doublet levels. Furthermore, in favorable nuclei such as ^{18}F,[6] ^{19}F,[7] and ^{21}Ne,[8] the PNC effects are enhanced by the fortuitous suppression of the parity-allowed γ decay [the $E1$ strength in ^{21}Ne is $\lesssim 8.5\cdot10^{-8}$ W.u. (Ref. 9)] relative to the parity-forbidden decay [the $M1$ strength in ^{18}F is 13 W.u. (Refs. 10 and 11)]. An understanding of the "two-level" nuclei ^{18}F, ^{19}F, and ^{21}Ne along with the somewhat more complicated case of the PNC α decay of the lowest 2^- $I=0$ level in ^{16}O (Ref. 12) is particularly important because their very different isospin properties permit us, in principle, to separately deduce the $\Delta I=0$ and $\Delta I=1$ PNC NN amplitudes: the PNC mixing in ^{16}O is $\Delta I=0$, in ^{18}F $\Delta I=1$, while ^{19}F and ^{21}Ne are mixtures of both $\Delta I=0$ and $\Delta I=1$ but with opposite relative signs.[13]

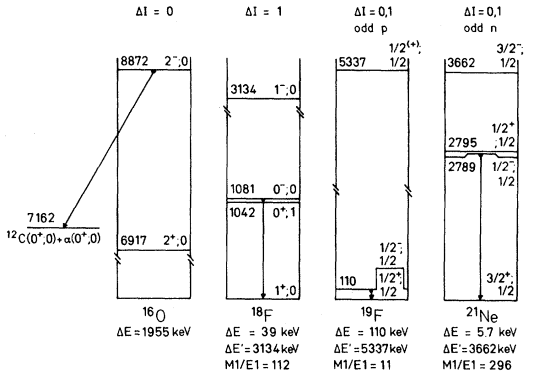

FIG. 1. Important examples of parity mixing in light nuclei. The level diagrams show the PNC transitions. The nearest opposite parity state whose admixture dominates the parity impurity is shown—ΔE is the splitting of this parity mixed doublet. The parity nonconservation in ^{18}F, ^{19}F, and ^{21}Ne is well approximated by two-level mixing. The nearest opposite parity level not included in the two-level approximation is shown in these cases—$\Delta E'$ is the splitting to that state. $M1/E1$ is an electromagnetic enhancement factor (see Sec. II B).

The major problem in extracting the elementary PNC NN amplitudes from the PNC effects in the "two-level" nuclei has been the difficulty and model dependence of the associated nuclear structure calculations. The many-body matrix elements of the PNC nucleon-nucleon potential must be calculable if we are to infer the strength of the underlying weak meson-nucleon coupling from the PNC observables. Our results suggest that this nuclear structure problem is much less tractable than originally hoped. The PNC potential is acutely sensitive both to the shape of the nuclear Fermi surface and, if transla-

tionally noninvariant shell model interactions are employed, to spurious center-of-mass motion.[14] These spurious components of the wave functions can be eliminated in complete $0\hbar\omega$ and $1\hbar\omega$ harmonic oscillator bases. However, since the infinite harmonic oscillator potential is too confining, still higher configurations must be included to soften the nuclear surface. For parity-changing observables the lowest order contributions of these higher configurations can be incorporated by including $2\hbar\omega$ excitations in the natural parity state. But even today, full $2\hbar\omega$ calculations for the light nuclei ^{18}F, ^{19}F, and ^{21}Ne tax or exceed the limits of feasibility.

However, in two cases—the parity-mixed 0^+-0^- doublet in ^{18}F and the $\frac{1}{2}^+$-$\frac{1}{2}^-$ doublet in ^{19}F—these structure uncertainties can be largely circumvented. In this paper we report studies of the β^+ decays of ^{18}Ne and ^{19}Ne with particular attention to the first-forbidden $0^+\rightarrow 0^-$ and $\frac{1}{2}^+\rightarrow\frac{1}{2}^-$ transitions which connect the isospin analog of one member of a parity-mixed doublet to the second member. These β transitions proceed dominantly through the axial charge component of the weak current. The strong pion exchange contribution to the axial charge operator is identical, apart from an isospin rotation and coupling constants, to the isovector PNC potential. Although the calculated *magnitude* of the exchange current matrix element is highly sensitive to nuclear structure assumptions, we will show that its *relative* contribution to the β-decay amplitude is remarkably model independent. Therefore, the measured β^+ decay rates can be combined with the observed parity mixing matrix elements in ^{18}F and ^{19}F to determine the strength of the pion-exchange PNC NN potential in a way which is insensitive to the choice of nuclear models. The results suggest that the parity mixing observed in light nuclei is consistent with the recent quark model estimates of the PNC meson-nucleon couplings made by Desplanques, Donoghue, and Holstein (DDH).[15]

However, the β-decay analogs of parity mixing cannot be measured in many interesting situations. How can we test the validity of shell model calculations for such cases? One approach is to make an omnibus comparison of measured and calculated γ-decay matrix elements for all low-lying transitions in the nuclei containing parity mixed doublets. We report comparisons of measured γ-ray observables in ^{18}F, ^{19}F, and ^{21}Ne with shell model calculations and investigate whether these less direct wave function tests also expose the shortcomings of the nuclear structure models. Such a comparison has already been presented by a Brookhaven group[13,16] for the case of ^{21}Ne using wave functions fairly similar to those we will discuss. It is particularly interesting to compare theory and experiment for γ-ray observables which connect the same pair of states (or their isospin analogs) involved in the parity mixing. This focuses on those states whose properties enter into the calculation of the PNC matrix element. The possible β- and γ-decay observables which correspond to the parity mixing in ^{16}O, ^{18}F, ^{19}F, and ^{21}Ne are listed in Table I. We find that the $0\hbar\omega+1\hbar\omega$ shell model predictions of the $E1$ γ-ray observables are not in quantitative agreement with the $A=19$ and $A=21$ data, and also systematically overestimate the absolute rates of the forbidden β^+ decays in $A=18$ and $A=19$.

The only calculation in accord with the results is one in $A=18$ utilizing a full $2\hbar\omega$ basis for the 0^+ state.[14] This convinces us that high-lying shell model configurations play a crucial role in PNC and $E1$ matrix elements. It is interesting that in both ^{18}Ne and ^{19}Ne, the measured β^+ decay rates are ~ 9 times slower than the full $0\hbar\omega$ and $1\hbar\omega$ shell model predictions. We argue that $2\hbar\omega$ excitations induce an "axial effective charge" for $A=18$ and $A=19$ that, in effect, reduces both the β decay and parity mixing matrix elements predicted by the $0\hbar\omega+1\hbar\omega$ shell model by a factor of ~ 3. In all cases the resulting matrix elements, when combined with the "best value" PNC meson-nucleon couplings of Desplanques, Donoghue, and Holstein,[15] predict PNC observables in light nuclei that agree well with the data.

II. EXPERIMENTAL PROCEDURE AND RESULTS

A. The gas transfer system

Since ^{18}Ne and ^{19}Ne are both noble gases that can easily be produced on gaseous targets, we constructed a rapid-cycling gas transport system to efficiently transfer the irradiated gas to a well-shielded counting station. The system, based on one previously designed at Chalk River,[17] is shown in the top portion of Fig. 2. One cycle of the system proceeds as

TABLE I. β and em decay analogs of the parity mixing in light nuclei.

	β decay	em decay
^{16}O	None	None[a]
^{18}F	^{18}Ne$\rightarrow$^{18}F(0^-)	None
^{19}F	^{19}Ne$\rightarrow$^{19}F($\frac{1}{2}^-$)	$E1$ ^{19}F($\frac{1}{2}^-$)$\rightarrow$^{19}F($\frac{1}{2}^+$)
^{21}Ne	None	$E1$ ^{21}Na($\frac{1}{2}^-$)$\rightarrow$^{21}Na($\frac{1}{2}^+$)

[a]Note that the $2^+I=0\leftrightarrow 2^-I=0$ $E1$ decays in ^{16}O which connect the same group of states involved in the parity mixing are not included since the $E1$ transitions are isospin forbidden and do not probe the $I=0$ components of the wave functions responsible for the PNC α decay.

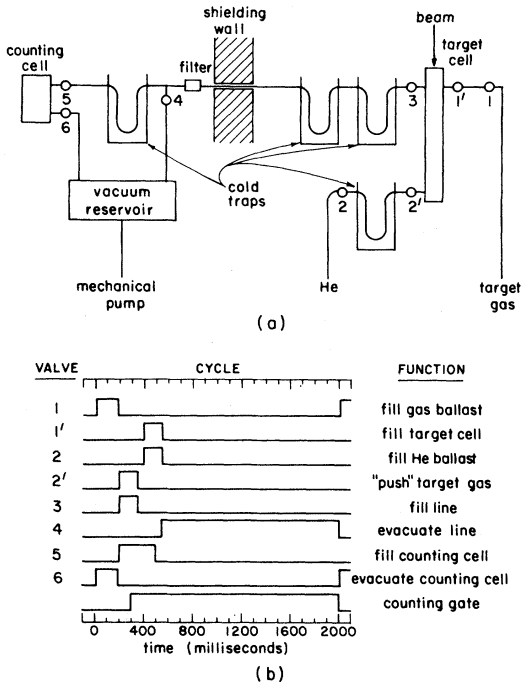

FIG. 2. Top: schematic diagram of the University of Washington gas transfer system. Bottom: the timing cycle used for the ^{18}Ne measurements.

follows. The target gas is admitted to an evacuated bombardment cell where it is irradiated for a time t_b by beams from the University of Washington FN tandem accelerator. Then the irradiated gas is propelled by a "piston" of He "pusher gas" from the bombardment cell, through a series of traps and filters designed to remove contaminant activities, to a heavily shielded counting station which was previously evacuated, where it is counted for a time t_c. The 11.43 cm-long bombardment cell has a 1.91 μm thick Ni entrance window and a Pt beam stop. The gas which flowed through Teflon tubing was controlled by electrically activated valves[18] controlled by an eight-channel digital sequencer. The purification system consisted of three LN_2 traps constructed of Cu tubing, the second of which was filled with a molecular sieve material. In addition a glass wool filter was used to remove any particulate impurities. The operating cycle used in the ^{18}Ne work is shown in the bottom portion of Fig. 2.

B. Details of the ^{18}Ne measurement

We produced ^{18}Ne via the ^{16}O(^{3}He,n) reaction on natural oxygen gas. A bombarding energy of 12.0 MeV was selected since good results were previously obtained[19] at this energy.

The main difficulty with the ^{18}Ne measurement was the intense background of 511 keV γ rays due to 110 min ^{18}F decays. This had two sources: ^{18}F produced via the ^{16}O(^{13}He,p) reaction and ^{18}F produced as a daughter in ^{18}Ne decays. The ^{18}F produced in the bombardment cell was essentially entirely removed by the first two cold traps since no discernible activity was ever detected in the third trap. A substantial fraction of the ^{18}F produced by ^{18}Ne decays within the counting chamber adhered to the walls of the chamber and could not be pumped away. We experimented with chamber ends made of lucite, Teflon, stainless steel, and Cu in an attempt to alleviate the problem. Lucite was better than the metals and similar to Teflon. We decided to use a lucite counting chamber because its low Z composition could minimize bremsstrahlung from energetic β particles that produce a background in the vicinity of the 1081 keV photopeak. The buildup of ^{18}F activity was reduced by removing the counting cell every hour or two and replacing it with one that had been washed. The counting chambers were cylindrical with inside diameter and length of 3.81 and 5.08 cm, respectively, and 1.9 cm walls. The performance of the gas transfer system could be monitored by multiscaling the annihilation radiation or by a pressure transducer[20] mounted in the counting cell. In order to optimize the counting rate of ^{18}Ne ($\tau = t_{1/2}/\ln 2 \sim 2.4$ sec) a 2.0 sec cycle ($t_b = 1.85$ sec, $t_c = 1.70$ sec) was chosen for the operating period of the gas transfer system.

Gamma rays were detected in a 27% Ge(Li) detector coaxial with the counting chamber. A 1.91 cm thick Pb slab interposed between the cell and the Ge(Li) detector preferentially absorbed the intense 511 keV radiation, thereby reducing the pileup background under the 1081 keV photopeak. This background was further reduced by pileup suppression circuitry. The cell and detector were surrounded by a Pb shield that attenuated room background. Two time-gated γ-ray spectra were accumulated. The first spectrum was accumulated for the first 0.85 sec after the counting cell was filled, the second spectrum for the following 0.85 sec. In this way some constraints could be placed on the half-lives of weak activities. A two-point spectrum stabilizer, operating on the Pb x rays and the 1042 keV photopeak, was employed.

The efficiency of the Ge(Li) detector plus Pb absorber was determined using radioactive sources that could be placed in various locations within the gas cell. Absolute γ intensities from calibrated ^{60}Co and ^{137}Cs sources along with relative intensities[21] from ^{207}Bi and ^{56}Co were used to obtain the efficiency data shown in Fig. 3. Because the Pb absorber causes the efficiency to fall drastically at low energies, the efficiency itself was not interpolated be-

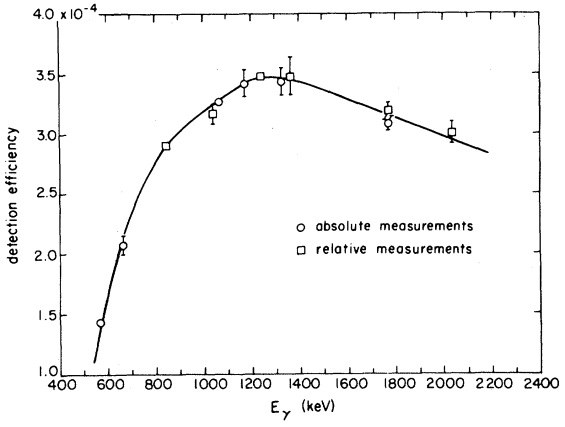

FIG. 3. Efficiency of the Ge(Li) detector and Pb absorber used for the ^{18}Ne measurements. When not shown the error bars are smaller than the symbols. The circles denote absolute calibrations, the squares relative ones.

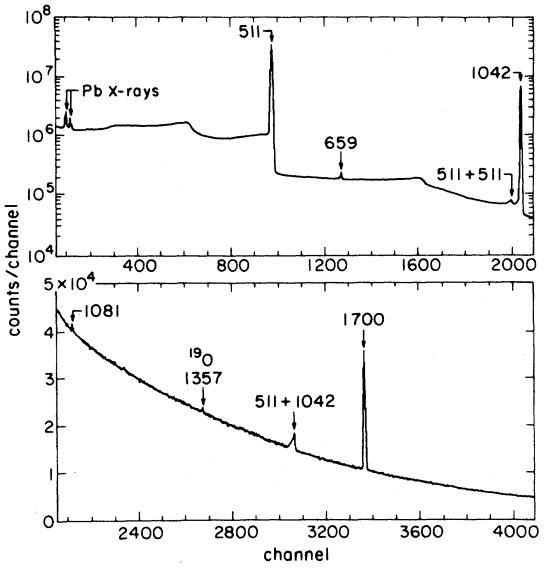

FIG. 4. Spectrum of γ rays following the β^+ decays of ^{18}Ne.

tween the calibration points to the energies needed for the ^{18}F measurement. Instead the efficiency was first divided by the calculated transmission of the Pb slab, the function was then interpolated, and the result multiplied by the calculated transmission of the Pb.

C. ^{18}Ne results

A spectrum of γ rays following the β^+ decay of ^{18}Ne (obtained by adding together the two time gated spectra mentioned above) accumulated in a 65 h run is shown in Figs. 4 and 5. This spectrum was taken with a more efficient and higher resolution detector than that used in our earlier work[22] and the present results supercede those given in Ref. 22. The energy scale in the spectrum was fixed by using the 659.26±0.20, 1041.55±0.08, and 1700.81±0.18 lines as calibrations, where the 659 keV γ ray comes from the 1700→1042 keV cascade transition. In addition to these lines, weak γ rays with energies of 1080.76±0.13 keV and 1357.05±0.16 keV were observed. The intensities of the various γ rays were extracted using a peak-fitting program. The shapes of the fitting function used on the 1081 and 1357 keV lines were determined by interpolation of the line shapes fitted to the strong transitions at 1042 and 1700 keV. The relative intensities of the 659, 1042, 1081, 1357, and 1700 keV γ rays in the two time-gated spectra are 0.786±0.014, 0.799±0.003, 0.784±0.130, 1.20±0.28, and 0.789±0.008, respectively. Clearly the 1081 keV γ-ray decays with a half-life consistent with ^{18}Ne while the 1357 keV γ-ray does not. Because of this, and the reasonable agreement of the measured energy with the accepted value[9] of 1080.54±0.12 keV, we ascribe the 1081 keV γ ray to β^+ decay of ^{18}Ne. From the observed separation of the 1081 and 1042 keV lines we find $\Delta E_x = 39.20 \pm 0.11$ keV for the splitting of the 0^- and 0^+ states in ^{18}F. The 1357 keV γ ray apparently arises from β^- decays of ^{19}O produced in the ^{19}O(^{3}He,2p) reaction. In an ancillary measurement with the gas transfer system operating on an 80 sec cycle, which greatly enhanced the strength of the

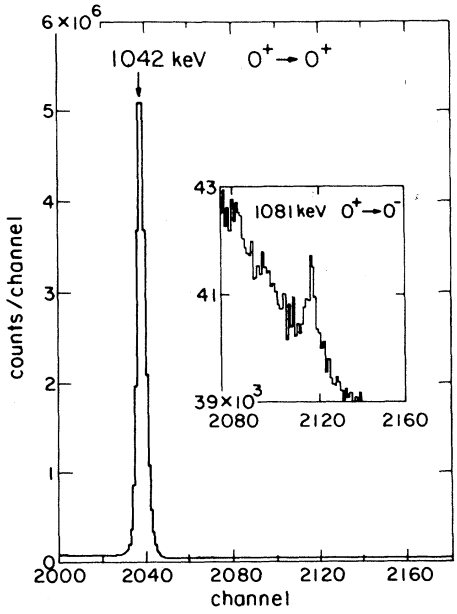

FIG. 5. Expanded spectrum showing the 1042 and 1081 keV photopeaks.

1357 keV γ rays compared to those from ^{18}Ne decays, we determined that the 1357 keV line decays with a half-life of 23.5±2.9 sec, close to the ^{19}O half-life of 26.9±0.08 sec. From analysis of the spectrum shown in Fig. 4 we obtain relative γ-ray intensities of 1.72±0.05, 100.0, $(2.89\pm0.26)\times10^{-2}$, and 0.687±0.013 for the 659, 1042, 1081, and 1700 keV γ rays, respectively. These results agree with our previous result[22] obtained by adding data from two smaller detectors except for the transition to the 1081 keV level, where the disagreement is ~2.5 times the combined errors. If instead of combining the spectra from both detectors in our previous experiment we had analyzed each detector separately we would have obtained $(2.59\pm0.53)\times10^{-2}$ and $(1.64\pm0.39)\times10^{-2}$ for the intensity of 1081 keV γ rays [normalized to $I(1042)=100.0$]. One of these results is in accord with our latest value. The other is unaccountably not. Our present result supercedes the previous one and is in agreement with recent measurements[23] at other laboratories. From the relative intensities of the 659, 1042, 1081, and 1700 keV γ rays we infer relative β branching ratios of

$$I_\beta(1042)=100.0\ ,$$

$$I_\beta(1081)=(2.94\pm0.26)\times10^{-2}$$

and

$$I_\beta(1700)=2.45\pm0.05$$

and a γ-ray branching ratio for the 1700 keV state

$$\mathrm{BR}(1700\rightarrow\text{g.s.}/1700\rightarrow\text{all})=0.285\pm0.007\ .$$

Our value for the γ branch from the 1700 keV level agrees well with a previous, less precise value[24] of 0.298±0.013. In computing the β branching ratio to the 1081 keV level we assumed that there was negligible feeding of the 1081 keV state by cascades from the 1700 keV level. The branch

$$\mathrm{BR}(1700\rightarrow1081/1700\rightarrow\text{all})$$

is known[24] to be less than 2×10^{-3}. We shall interpret this conservatively as a $(1\pm1)\times10^{-3}$ branch. In that case

$$I_\beta(1081)=(2.70\pm0.36)\times10^{-2}\ .$$

Our results are compared to previous work in Table II.

D. *ft* values for ^{18}Ne β^+ decay

The energy release in the ^{18}Ne β^+ decay to the ^{18}F ground state is 3425±5 keV.[25] Computing the phase space factor f according to the prescription of Wilkinson and Macefield[26] we find f values of 687.1±4.5, 136.8±1.3, 127.3±1.2, and 33.7±0.4 sec for transitions to the ground, 0^+, 0^-, and 1^+ states, respectively. We computed f assuming an allowed shape in all cases. It will be argued below that it is a reasonable first approximation to use an allowed shape for the first forbidden transition since the dominant axial charge operator is independent of the momentum transferred to the leptons.

TABLE II. (A) Relative γ-ray intensities observed in the β^+ decay of ^{18}Ne. (B) β^+ intensities in the decay of ^{18}Ne.

(A)

E_x	This work	Hardy *et al.* (Ref. 19)	Aslanides *et al.*[a]	Hernandez and Daehnick[b]
659	1.72 ±0.05	2.1 ±0.3	1.6 ±0.5	1.69 ±0.04
1042	100.	100.	100.	100.
1081	$(2.89\pm0.26)\times10^{-2}$			$(2.97\pm0.22)\times10^{-2}$
1700	0.687±0.013	0.71±0.17	0.72±0.21	0.646±0.021

(B)

	$I(\beta^+)$		logft (sec)	
E_x	This work[c]	Hardy *et al.* (Ref. 19)	This work[d]	Hardy *et al.* (Ref. 19)
0	92.11 ±0.21	92.11±0.21	3.096±0.004	3.088±0.003
1042	7.70 ±0.21	7.66±0.21	3.473±0.013	3.468±0.013
1081	$(2.07\pm0.28)\times10^{-3}$		7.012±0.059	
1700	0.188±0.006	0.23±0.03	4.477±0.015	4.38 ±0.05

[a]E. Aslanides, F. Jundt, and A. Gallman, Nucl. Phys. A152, 251 (1972).
[b]Reference 23.
[c]Normalized to Ref. 19 as discussed in text.
[d]Based on adopted value $t_{1/2}=1.672\pm0.008$ sec (see text).

There are two recent precise measurements of $t_{1/2}$ for ^{18}Ne, 1.687±0.009 sec (Ref. 19) and 1.669±0.004 sec.[27] Since these do not agree within the stated errors we arbitrarily double the formal error on the combined result to obtain

$$t_{1/2}=1.672\pm0.008 \text{ sec} .$$

We convert our relative γ-ray branching ratios into absolute ones by using the previously determined ratio[19] of

$$R=(7.83\pm0.21)\times10^{-2}$$

1042 keV γ rays per ^{18}Ne β^+ decay. Then the absolute β^+ branching ratios (in percent) can be determined from relations such as

$$\mathrm{BR}(\beta^+\rightarrow1042)=R\,[I_\gamma(1042)-I_\gamma(659)] ,$$

where I_γ refers to our relative γ-ray intensities normalized to $I_\gamma(1042)=100$. The results and the corresponding ft values are displayed in Table II along with some recent results from our laboratories.

E. First forbidden β^+ decays of ^{19}Ne: Experimental details and results

We produced the ^{19}Ne activity via the ^{19}F(p,n) reaction on SF_6 gas. The bombarding energy of 6.4 MeV was chosen to lie below the threshold for the (p,n) reactions on ^{32}S, ^{33}S, and ^{34}S. In addition the proton energy was low enough so that the neutrons from ^{19}F(p,n) did not have enough energy to produce ^{19}O via the ^{19}F(n,p) reaction. Since no background activity was detected we did not cool the traps for the ^{19}Ne measurement. A 20.0 sec cycle ($t_b=19.8$ sec, $t_c=19.7$ sec) was used in the gas transport system. Since the γ ray following the decay to the $\frac{1}{2}^-$ level has an energy of only 110 keV and the β^+ end point is lower than in the ^{18}Ne$\rightarrow^{18}$F (g.s) decay, a lucite counting cell was constructed having the same internal dimensions as that used in the ^{18}Ne work but with thinner walls (9.5 mm). The intense background of 511 keV quanta that would have obscured the weak 110 keV peak was effectively removed by a coincidence gate. Nuclear γ rays detected in a 15% Ge(Li) detector equipped with pileup rejection circuitry were counted in coincidence with 511 keV quanta detected in each of two back-to-back 7.6 cm×7.6 cm NaI detectors. The geometry is shown in Fig. 6. A time-to-amplitude converter (TAC) was started on fast twofold coincidences between 511 keV events in the two NaI detectors and a fast trigger from the Ge(Li) detector. Four-parameter data, pulse heights in all three detectors and the TAC signal, were recorded in event-by-event mode and analyzed in subsequent

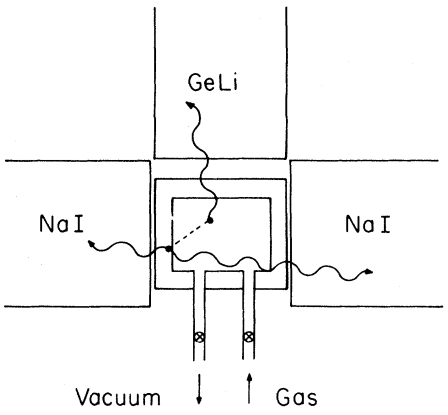

FIG. 6. Schematic diagram of the ^{19}Ne first forbidden decay measurements.

playback. A time resolution of $\lesssim$20 nsec at ~110 keV was achieved, yielding a real-to-random ratio of ~3.8. A spectrum of coincident events in the Ge(Li) detector before and after subtraction of random coincidences is shown in Fig. 7. A clear photopeak at 110.0±0.3 keV is observed along with a bremsstrahlung continuum. Since these data have already been reported[28] we merely summarize the results in this paper. The 110 keV peak corresponds to a branching ratio of $(1.20\pm0.20)\times10^{-4}$ for the ^{19}Ne$\rightarrow^{19}$F($\frac{1}{2}^-$) decay.

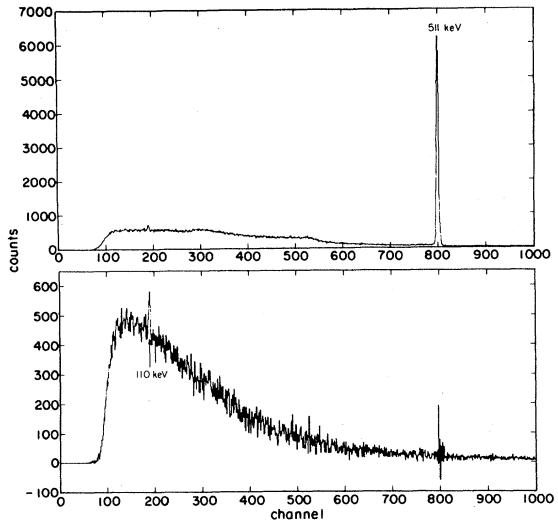

FIG. 7. Gamma-ray spectra in the 15% Ge(Li) detector following the β^+ decays of ^{19}Ne. Spectra are in coincidence with 511 keV photons detected in two NaI detectors. Top: real plus random coincidences. Bottom: real coincidences with randoms subtracted.

F. ^{19}Ne β^+ decays to ^{19}F($\frac{3}{2}^+$): Experimental details and results

Interest in the ^{19}Ne β^+ transition to the 1554 keV $\frac{3}{2}^+$ state of ^{19}F was originally stimulated by a suggestion[29] that inelastic ν scattering on ^{19}F to the 1554 keV level would be a practical way to study neutral weak currents. The β^+ decay rate was needed to calculate the ^{19}F(ν,ν') cross section. Two discordant measurements for this branching ratio have been reported: $(8.2\pm2.0)\times10^{-6}$ by Freedman *et al.*[30] and $(2.1\pm0.3)\times10^{-5}$ by Alburger.[31] Although the recent extensive data in inelastic ν scattering have removed much of the original interest in this transition we decided to remeasure this branch as a byproduct of our work on first-forbidden β^+ decays in ^{19}Ne.

The ^{19}Ne activity was produced as described above. A thicker-walled counting cell used in the ^{18}Ne work was employed. A 9.2% Ge(Li) detector coaxial with the counting cell viewed the ^{19}Ne activity through a 2.4 cm thick Pb slab that reduced the intense 511 keV radiation relative to the 1357 keV radiation expected from the decay of the 1554 keV level. Pileup was reduced by rejection circuitry. A ^{60}Co source was placed near the counting cell to provide an energy calibration and to fix one of the points of the gain stabilizer, the other being set on the 72.8 and 75 keV Pb x-ray peaks. In all other respects the setup is similar to that used in the ^{18}Ne work. The detection efficiency at 1357 and 511 keV was determined using ^{7}Be, ^{22}Na, ^{54}Mn, ^{56}Co, ^{60}Co, ^{137}Cs, and ^{207}Bi radioactive sources. Finite solid angle effects were included by placing the sources in various positions within the counting cell and averaging the results. A gamma ray spectrum based on ~24 h of running is shown in Fig. 8. A clear photopeak is observed at 1356.84 ± 0.13 keV in good agreement with the expected value[9] of 1357.0 ± 0.2 keV. The ratio of intensities at 1357 and 511 keV is $(5.47\pm0.53)\times10^{-5}$. Taking into account the 5% of the positrons which are annihilated in flight, the 92.5% branching ratio of the 1554 keV level to the 197 keV state, and the fact that two annihilation quanta are emitted per β^+ decay, we obtain a branching ratio for ^{19}Ne β^+ decay to ^{19}F($\frac{3}{2}^+$) of $(2.34\pm0.30)\times10^{-5}$. This result is in excellent agreement with the value $(2.1\pm0.3)\times10^{-5}$ reported by Alburger[31] and disagrees strongly with that given in Ref. 30.

G. *ft* values for ^{19}Ne β^+ decays

The energy release in ^{19}Ne β^+ decay to the ^{19}F ground state is 2216.3 ± 0.6 keV.[25] We take the excitation energies of the $\frac{1}{2}^-$ and $\frac{3}{2}^+$ states to be 109.9 (Ref. 9) and 1555.0 ± 0.2 keV, respectively, where the latter value was obtained by adding the energy of the $\frac{3}{2}^+\rightarrow\frac{5}{2}^+$ γ ray given in Ref. 31 to the excitation energy of the $\frac{5}{2}^+$ state given in Ref. 9. Assuming all three transitions have an allowed shape (it will be argued below that an allowed shape is a reasonable first approximation for the $\frac{1}{2}^+\rightarrow\frac{1}{2}^-$ transition since the dominant axial charge operator is independent of the momentum transfer to the leptons) we compute the phase space factors f according to the prescription of Wilkinson and Macefield.[26] There is disagreement among the recent measurements of $t_{1/2}$ for ^{19}Ne decay, 17.36 ± 0.06,[32] 17.36 ± 0.06,[33] 16.72 ± 0.05,[34] 17.43 ± 0.06,[35] and 17.219 ± 0.017 sec.[36] Since the quoted errors are not consistent with the spread of the values we arbitrarily omit the highly discordant value of Ref. 34 and weight the remaining measurements equally to obtain $t_{1/2}=17.34\pm0.09$ sec, where the error is the standard deviation of the individual results. We assume branching ratios of 0.9999, $(1.2\pm0.2)\times10^{-4}$, and $(2.22\pm0.21)\times10^{-5}$ for transitions to the $\frac{1}{2}^+$, $\frac{1}{2}^-$, and $\frac{3}{2}^+$ states, respectively, where the last value was obtained by combining our result with that of Ref. 31. The corresponding *ft* values are 1727 ± 9, $(1.15\pm0.19)\times10^7$, and $(5.01\pm0.47)\times10^5$ sec, respectively. Results are summarized in Table III.

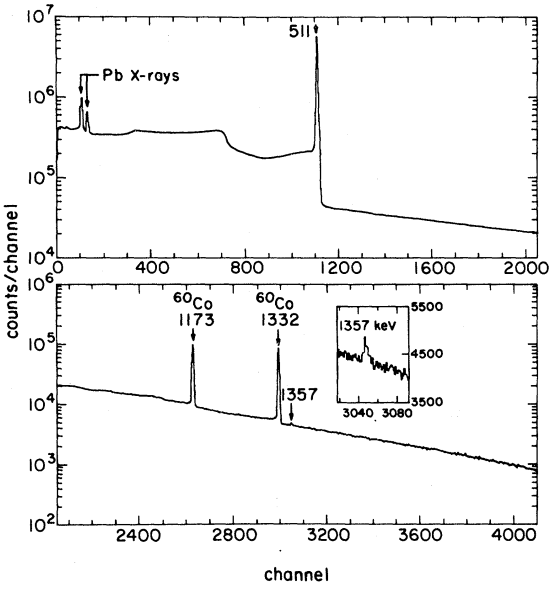

FIG. 8. Singles spectrum of γ rays following the β^+ decays of ^{19}Ne along with a ^{60}Co source used for calibration.

III. DISCUSSION

A. First forbidden β decays of ^{18}Ne and ^{19}Ne

The general result for the differential $\beta^{\pm}$ decay rate for the decay of an unpolarized nucleus $J_i \to J_f$ is[37]

$$
\begin{aligned}
d\omega^{\mp} = & \frac{2}{\pi^2} G_F^2 \beta \epsilon^2 (W_0 - \epsilon)^2 \mathcal{F}(Z,\epsilon) \frac{1}{2J_i+1} \\
& \times \int \frac{d\Omega_\nu}{4\pi} \int \frac{d\Omega_k}{4\pi} \left\{ \sum_{J=0}^{\infty} [(1+\hat{\nu}\cdot\vec{\beta}) \,|\, \langle J_f || \hat{\mathscr{M}}_J || J_i \rangle \,|^2 \right. \\
& \quad + (1 - \hat{\nu}\cdot\vec{\beta} + 2(\hat{\nu}\cdot\hat{q})(\hat{q}\cdot\vec{\beta})) \,|\, \langle J_f || \hat{\mathscr{L}}_J || J_i \rangle \,|^2 \\
& \quad - \hat{q}\cdot(\hat{\nu}+\vec{\beta}) 2\,\mathrm{Re}(\langle J_f || \hat{\mathscr{L}}_J || J_i \rangle \langle J_f || \hat{\mathscr{M}}_J || J_i \rangle^*)] \\
& + \sum_{J=1}^{\infty} [(1 - (\hat{\nu}\cdot\hat{q})(\hat{q}\cdot\vec{\beta}))(\,|\, \langle J_f || \hat{\mathscr{T}}^{\mathrm{el}}_J || J_i \rangle \,|^2 + \,|\, \langle J_f || \hat{\mathscr{T}}^{\mathrm{mag}}_J || J_i \rangle \,|^2) \\
& \quad \left. \pm \hat{q}\cdot(\hat{\nu}-\vec{\beta}) \, 2\,\mathrm{Re}(\langle J_f || \hat{\mathscr{T}}^{\mathrm{mag}}_J || J_i \rangle \langle J_f || \hat{\mathscr{T}}^{\mathrm{el}}_J || J_i \rangle^*)] \right\} \qquad (1)
\end{aligned}
$$

with G_F the weak coupling constant, $(\epsilon, \vec{k})$ the electron four-momentum, $\vec{\beta} \equiv \vec{k}/\epsilon$, $\hat{\nu} = \vec{\nu}/|\vec{\nu}|$ the unit vector in the direction of the neutrino, $\vec{q} = \vec{k} + \vec{\nu}$ the nuclear three-momentum transfer, W_0 the maximum electron energy, and $\mathcal{F}(Z,\epsilon)$ a correction for the distortion of the electron wave function in the Coulomb field of the daughter nucleus of charge Z. We take $\mathcal{F}$ from numerical solutions of the Dirac equation tabulated in Ref. 38. The charge, longitudinal, transverse electric, and transverse magnetic multipole operators

$$
\begin{aligned}
& \hat{\mathscr{M}}_{JM} \equiv \hat{M}_{JM} + \hat{M}^5_{JM} \equiv \int d\vec{x}\, M_J(\vec{x}) \hat{\mathscr{J}}^M_0(\vec{x}) \,, \\
& \hat{\mathscr{L}}_{JM} \equiv \hat{L}_{JM} + \hat{L}^5_{JM} \equiv i \int d\vec{x} \left[\frac{1}{q} \vec{\nabla} M^M_J(\vec{x}) \right] \cdot \hat{\vec{\mathscr{J}}}(\vec{x}) \,, \qquad (2) \\
& \hat{\mathscr{T}}^{\mathrm{el}}_{JM} \equiv \hat{T}^{\mathrm{el}}_{JM} + \hat{T}^{\mathrm{el5}}_{JM} \\
& \qquad \equiv i \int d\vec{x} \left[\frac{1}{q} \vec{\nabla} \times \vec{\mathrm{M}}^M_{JJ}(\vec{x}) \right] \cdot \hat{\vec{\mathscr{J}}}(\vec{x}) \,, \\
& \hat{\mathscr{T}}^{\mathrm{mag}}_{JM} \equiv \hat{T}^{\mathrm{mag}}_{JM} + \hat{T}^{\mathrm{mag5}}_{JM} \equiv \int d\vec{x}\, \vec{\mathrm{M}}^M_{JJ}(\vec{x}) \cdot \hat{\vec{\mathscr{J}}}(\vec{x})
\end{aligned}
$$

are formed from the weak hadronic current operator

$$
\hat{\mathscr{J}}_\mu = \hat{J}_\mu + \hat{J}^5_\mu \qquad (3)
$$

which contains, in principle, one-, two- through A-body components. All axial-vector quantities are distinguished from vector quantities by the superscript 5. The multipole operators in Eqs. (2) are defined in terms of the projection functions

$$
\begin{aligned}
& M^M_J(\vec{x}) \equiv j_J(qx) Y^M_J(\Omega_x) \,, \\
& \vec{\mathrm{M}}^M_{JL}(\vec{x}) \equiv j_L(qx) \vec{\mathrm{Y}}^M_{JL1}(\Omega_x) \,.
\end{aligned} \qquad (4)
$$

This analysis simplifies considerably for the transition

$$
^{18}\mathrm{Ne}\ (J^\pi T = 0^+ 1) \to {}^{18}\mathrm{F}(0^- 0) \,.
$$

The spin and parity selection rules eliminate all but two operators,

$$
\begin{aligned}
\hat{M}^5_{00} &= \int d\vec{x}\, M^0_0(\vec{x}) \hat{J}^5_0(\vec{x}) \\
&\underset{q\to 0}{\to} \frac{1}{\sqrt{4\pi}} \int d\vec{x}\, \hat{J}^5_0(\vec{x}) \\
\hat{L}^5_{00} &= i \int d\vec{x} \left[\frac{1}{q} \vec{\nabla} M^0_0(\vec{x}) \right] \cdot \hat{\vec{J}}^5(\vec{x}) \\
&\underset{q\to 0}{\to} \frac{iq}{6\sqrt{4\pi}} \int d\vec{x}\, x^2 \vec{\nabla} \cdot \hat{\vec{J}}^5(\vec{x})
\end{aligned} \qquad (5)
$$

with only the axial-charge operator $\hat{M}^5_{00}$ contributing in the long-wavelength limit. Four additional operators contribute to the

$$
^{19}\mathrm{Ne}(\tfrac{1}{2}^+ \tfrac{1}{2}) \to {}^{19}\mathrm{F}(\tfrac{1}{2}^- \tfrac{1}{2})
$$

decay:

$$
\begin{aligned}
& \hat{M}_{1M} \underset{q\to 0}{\to} \frac{q}{3} \int d\vec{x}\, x Y_{1M}(\Omega_x) \hat{J}_0(\vec{x}) \,, \\
& \hat{L}_{1M} \underset{q\to 0}{\to} \frac{q_0}{q} \hat{M}_{1M} \,, \\
& \hat{T}^{\mathrm{el}}_{1M} \underset{q\to 0}{\to} \frac{q_0}{q} \sqrt{2} \hat{M}_{1M} \,, \\
& \hat{T}^{\mathrm{mag5}}_{1M} \underset{q\to 0}{\to} \frac{iq}{2\sqrt{6\pi}} \int d\vec{x} [\vec{x} \times \hat{\vec{J}}^5(\vec{x})]_M \,,
\end{aligned} \qquad (6)
$$

where we have used current conservation to relate L_{1M} and $T^{\rm el}_{1M}$ to the vector charge operator M_{1M}. As these additional operators vanish as $q_\mu \to 0$, we expect the axial charge operator to dominate the ^{19}Ne $\frac{1}{2}^+ \to \frac{1}{2}^-$ transition as well. This expectation is confirmed by the detailed calculations discussed below.

The strength of the forbidden vector current multipole matrix elements in Eqs. (6) is fixed, through the conserved vector current (CVC) hypothesis, by known γ-decay rates of the corresponding $E1$ transitions in ^{19}Ne and ^{19}F (see Fig. 9). The γ-decay rate for a $\frac{1}{2}^- \to \frac{1}{2}^+$ transition is

$$\omega_\gamma = \frac{8\pi\alpha q}{2J_i+1} |\langle \tfrac{1}{2}^+ || \hat{T}^{{\rm el};\gamma} || \tfrac{1}{2}^- \rangle|^2 , \tag{7}$$

where $\hat{T}^{{\rm el};\gamma}_{JM}$ is defined as in Eqs. (2), but with the electromagnetic hadronic current operator

$$\hat{J}^\gamma_\mu = \hat{J}^S_\mu + \hat{J}^{V_3}_\mu \tag{8}$$

in place of the weak hadronic current operator $\hat{J}_\mu$. The conserved vector current hypothesis[39] relates the isovector component of the electromagnetic current to the vector weak current $\hat{J}_\mu$ by

$$\hat{J}^\pm_\mu = \hat{J}^{V_1}_\mu \pm i\hat{J}^{V_2}_\mu , \tag{9}$$

where $\hat{J}^{V_3}_\mu$ represents the third component of the isovector current $\hat{J}^{\vec{V}}_\mu$, etc. Thus, to the extent that the nuclear states have good isospin, the many-body matrix elements of the weak operator $T^{\rm el}_{J=1}$ (and thus of L_1 and M_1) can be determined from the experimental γ-decay rates in ^{19}Ne and ^{19}F. We find

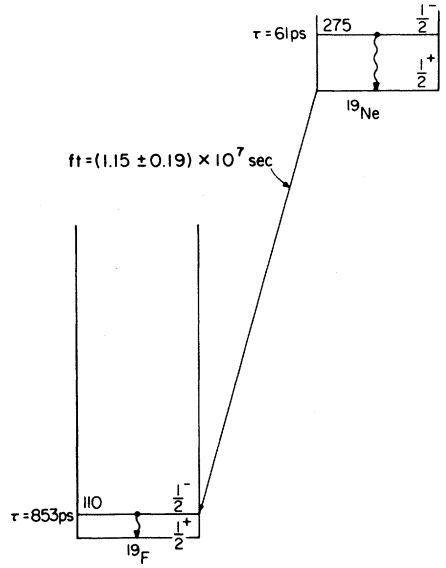

FIG. 9. Corresponding β^+ (first forbidden) and $\gamma(E1)$ decays between the $\frac{1}{2}^+$ and $\frac{1}{2}^-$ levels in ^{19}F and ^{19}Ne.

$$\begin{aligned}
\langle \tfrac{1}{2}^+ || T^{\rm el}_1/q || \tfrac{1}{2}^- \rangle_{^{19}{\rm Ne}\to{}^{19}{\rm F}} &= \langle \tfrac{1}{2}^+ || T^{{\rm el};\gamma}_1/q || \tfrac{1}{2}^- \rangle_{^{19}{\rm Ne}} - \langle \tfrac{1}{2}^+ || T^{{\rm el};\gamma}_1/q || \tfrac{1}{2}^- \rangle_{^{19}{\rm F}} \\
&= \pm(1.55\pm0.03)\times10^{-4} , \\
2\langle \tfrac{1}{2}^+ || T^{\rm el}_{1;T=0}/q || \tfrac{1}{2}^- \rangle &= \langle \tfrac{1}{2}^+ || T^{{\rm el};\gamma}_1/q || \tfrac{1}{2}^- \rangle_{^{19}{\rm Ne}} + \langle \tfrac{1}{2}^+ || T^{{\rm el};\gamma}_1/q || \tfrac{1}{2}^- \rangle_{^{19}{\rm F}} \\
&= \mp(0.07\pm0.03)\times10^{-4} ,
\end{aligned} \tag{10}$$

where the momentum transfer q must be evaluated for the indicated transitions. Note that the isoscalar $E1$ operator, which contributes only to the electromagnetic rates, is almost zero. This is expected since it corresponds, in the $q \to 0$ and good isospin limits, to an excitation of the nuclear center of mass.

We now focus on the one- and two-body contributions to the dominant operator, the axial charge. The one-body contribution is obtained from the nonrelativistic reduction of the axial current for a free nucleon. To $O(1/M)$ one finds[37,40]

$$\hat{J}^{5\pm}_{0(1)} = F_A \sum_{i=1}^{A} \tau_\pm \left[\vec{\sigma}(i)\cdot\frac{\vec{p}(i)}{2M}\delta(\vec{x}-\vec{x}_i) + \delta(\vec{x}-\vec{x}_i)\frac{\vec{p}(i)}{2M}\cdot\vec{\sigma}(i) \right]$$

$$-i\left[H, \frac{F_p}{2M}\vec{\nabla}\cdot\sum_{i=1}^{A}\vec{\sigma}(i)\tau_\pm(i)\delta(\vec{x}-\vec{x}_i) \right] , \tag{11}$$

where H is the nuclear Hamiltonian and $F_A = -1.25$. We use the partial conservation of axial-vector current (PCAC) value $F_P = 2MF_A/m_\pi{}^2$ for the pseudoscalar coupling constant. The first term in Eq. (11), although forbidden in the sense that $|\vec{p}(i)|/M \sim \frac{1}{5}$, is finite as $q \to 0$ while the second term does not contribute to $\hat{M}^5_{00}$ in the long wavelength limit.

The two-body contribution to the axial charge operator is dominated by pion exchange (see Fig. 10). This (and the π-exchange contribution to the space component of the vector current) can be computed from a low-energy theorem based on the partial conservation of the axial-vector current and current algebra.[41] For J_0^5 the result, to leading order in $(1/M)$, is given entirely by the seagull term

$$\hat{J}^{5\pm}_{0(2)} = -\frac{m_\pi{}^2 g_{\pi NN}{}^2 F_1^v}{8\pi M^2 F_A}\frac{1}{2}\sum_{\substack{ij\\ i\neq j}}[\tau(i)\times\tau(j)]_\pm[\vec{\sigma}(i)\cdot\hat{r}_{ij}\delta(\vec{x}-\vec{x}_j)+\vec{\sigma}(j)\cdot\hat{r}_{ij}\delta(\vec{x}-\vec{x}_i)]\phi(m_\pi r_{ij}) , \tag{12}$$

where $\vec{r}_{ij}=\vec{r}_i-\vec{r}_j$, $[\ \ ]_\pm\equiv\frac{1}{2}([\ \ ]_1\pm i[\ \ ]_2)$, $\phi(x)=(e^{-x}/x)(1+1/x)$, and the vector form factor $F_1^v=1$. As the one-pion-exchange current is of the *same order* ($|\vec{p}|/M\sim v/c$) as the one-body contribution, it is expected to be important in axial charge transitions.[41]

B. Parity mixing in ^{18}F, ^{19}F, and ^{21}Ne

Nuclear properties of the "two-level" parity mixed doublets of ^{18}F, ^{19}F, and ^{21}Ne are illustrated in Fig. 1. The circular polarization of the γ rays emitted in the

$$J^\pi T = 0^-0\ (1.08\ \text{MeV}) \rightarrow 1^+0\ (0.0\ \text{MeV})$$

transition in ^{18}F has been measured by three different groups.[6,42,43] The results, which are mutually consistent, can be combined to yield

$$P_\gamma\ (1.08\ \text{MeV}) = (-0.8\pm1.2)\times10^{-3} .$$

This provides an upper limit on the magnitude of the matrix element of the $\Delta I=1$ PNC interaction which mixes the initial state with the nearby 0^+1 (1.04 MeV) level. In the two level mixing approximation,[44]

$$P_\gamma\ (1.08\ \text{MeV}) = \frac{2}{\Delta E}\,\text{Re}\left[\frac{\langle 1^+||T_1^{\text{mag};\gamma}||0^+\rangle}{\langle 1^+||T_1^{\text{el};\gamma}||0^-\rangle}\times\langle 0^+1\,|\,V_{\text{PNC}}\,|\,0^-0\rangle\right] , \tag{13}$$

with $\Delta E=39.2\pm0.1$ keV and with the electromagnetic multipole operators evaluated at a momentum transfer $q=1.08$ MeV/c. The magnitude of the ratio of reduced matrix elements,

$$\left|\frac{\langle 1^+||T_1^{\text{mag};\gamma}||0^+\rangle}{\langle 1^+||T_1^{\text{el};\gamma}||0^-\rangle}\right| = 111\pm8 ,$$

is determined by the lifetimes of the 0^+ and 0^- states, 2.5 ± 0.3 fsec (Refs. 10 and 11) and 27.5 ± 1.9 psec (Ref. 9), respectively. The strong isospin hindrance of the $E1$ matrix element, which accounts for this favorable ratio, probably rules out any convincing theoretical calculation of the sign of P_γ.

The PNC asymmetry A_γ of the 110 keV γ ray emitted in the decay of the polarized first excited state of ^{19}F has been measured by two groups.[7,59] The results,

$$A_\gamma = (-8.5\pm2.6)\times10^{-5}$$

and

$$A_\gamma = (-4.5\pm3.6)\times10^{-5} ,$$

can be combined to yield

$$A_\gamma = (-7.1\pm2.1)\times10^{-5} ,$$

where

$$d\omega/d\Omega_\gamma \sim 1+A_\gamma\cos\theta$$

for a completely polarized $\frac{1}{2}^-$ state. In the two-level mixing approximation A_γ probes a combination of $I=0$ and $I=1$ components of the PNC interaction responsible for the mixing of the $\frac{1}{2}^-\frac{1}{2}$ level with the $\frac{1}{2}^+\frac{1}{2}$ ground state,[7,44]

$$A_\gamma\ (110\ \text{keV}) = \frac{2}{\Delta E}\,\text{Re}\left[\frac{\langle\frac{1}{2}^+||T_1^{\text{mag};\gamma}||\frac{1}{2}^+\rangle-\langle\frac{1}{2}^-||T_1^{\text{mag};\gamma}||\frac{1}{2}^-\rangle}{\langle\frac{1}{2}^+||T_1^{\text{el};\gamma}||\frac{1}{2}^-\rangle}\langle\tfrac{1}{2}^+\tfrac{1}{2}\,|\,V_{\text{PNC}}\,|\,\tfrac{1}{2}^-\tfrac{1}{2}\rangle\right] \tag{14}$$

with $\Delta E=110$ keV and with the operators evaluated at $q=110$ keV/c. The measured ground state magnetic moment, 2.6289,[9] yields

$$\langle\tfrac{1}{2}^+||T_1^{\text{mag};\gamma}||\tfrac{1}{2}^+\rangle = i\,8.69\times10^{-5} ,$$

and the lifetime of the $\frac{1}{2}^-$ level, 853 ± 10 psec, gives

$$|\langle\tfrac{1}{2}^+||T_1^{\text{el};\gamma}||\tfrac{1}{2}^-\rangle| = 0.88\times10^{-5} .$$

Although the magnetic moment of the $\frac{1}{2}^-$ level is

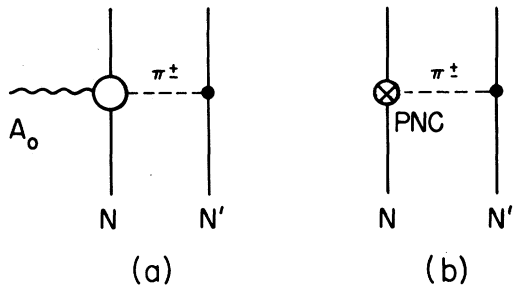

FIG. 10. Pion exchange current contributions to the axial charge operator and to the PNC *NN* force.

not known, several recent shell model calculations[44] predict values between -0.17 and -0.24. The consistency of these results and the large value of $\mu(\frac{1}{2}^+)/\mu(\frac{1}{2}^-)$ indicates that the lack of a measurement of $\mu(\frac{1}{2}^-)$ is unlikely to affect the quality of theoretical predictions of A_γ. The sign of A_γ is dependent on that of the $E1$ matrix element; although this transition is weak ($1.2\cdot10^{-3}$ W.u.), the suppression is much less severe than for the $E1$ transition in ^{18}F, so that the $E1$ sign may be calculable. All three shell model calculations we discuss below predict a negative A_γ and magnitudes of the $E1$ matrix element not too much larger than experiment.

The PNC circular polarization of the γ rays from the

$$\tfrac{1}{2}^-\tfrac{1}{2}\ (2.789\ \text{MeV})\rightarrow\tfrac{3}{2}^+\tfrac{1}{2}$$

transition in ^{21}Ne has been measured by a Seattle–Chalk River collaboration.[8] The upper limit obtained is

$$P_\gamma\ (2.80\ \text{MeV})=(0.8\pm1.4)\cdot10^{-3}\ .$$

This experiment is sensitive to a combination of $I=0$ and $I=1$ components of the PNC potential governing the mixing of the $\frac{1}{2}^-\frac{1}{2}$ and nearby $\frac{1}{2}^+\frac{1}{2}$ (2.796 MeV) levels. However, because ^{21}Ne is an odd-neutron rather than odd-proton nucleus, the relative sign of these isospin components differs from that in ^{19}F. The experimental limit is significant because it indicates a PNC matrix element much smaller than found in ^{19}F, and so fixes the relative sign of the dominant isovector and isoscalar PNC couplings. The expression for P_γ, in the two level mixing approximation, is[44]

$$P_\gamma\ (2.789\ \text{MeV})=-\frac{2}{\Delta E}\frac{1+\delta_-^*\delta_+}{1+|\delta_-|^2}\ \text{Re}\left[\frac{\langle\frac{3}{2}^+||T_1^{\text{mag};\gamma}||\frac{1}{2}^+\rangle}{\langle\frac{3}{2}^+||T_1^{\text{el};\gamma}||\frac{1}{2}^-\rangle}\langle\tfrac{1}{2}^+\tfrac{1}{2}\,|\,V_{\text{PNC}}\,|\,\tfrac{1}{2}^-\tfrac{1}{2}\rangle\right] \tag{15}$$

with $\Delta E=5.74\pm0.15$ keV,[11]

$$\delta_-=\langle\tfrac{3}{2}^+||T_2^{\text{mag};\gamma}||\tfrac{1}{2}^-\rangle/\langle\tfrac{3}{2}^+||T_1^{\text{el};\gamma}||\tfrac{1}{2}^-\rangle\ ,$$

and

$$\delta_+=\langle\tfrac{3}{2}^+||T_2^{\text{el};\gamma}||\tfrac{1}{2}^+\rangle/\langle\tfrac{3}{2}^+||T_1^{\text{mag};\gamma}||\tfrac{1}{2}^+\rangle\ .$$

All multipole operators are evaluated at $q=2.789$ MeV/c. The measured partial lifetimes are $\tau_+=7.6\pm0.8$ fsec (Refs. 11 and 16) and $\tau_-=696\pm51$ psec.[9] A limit of $|\delta_+|<0.39$ can be obtained from the measured lifetime of the $\frac{1}{2}^+$ level and the extreme assumption that $B(E2)=30$ W.u., while a shell model calculation predicts $\delta_+=i0.026$. The extreme weakness of the $\frac{1}{2}^-\rightarrow\frac{3}{2}^+$ decay discourages attempts to calculate δ_- or the sign of $\langle\frac{3}{2}^+||T_1^{\text{el};\gamma}||\frac{1}{2}^-\rangle$. However, a recent measurement[45] of the pair emission for the transition $\frac{1}{2}^-\rightarrow\frac{3}{2}^+$ determined $|\delta_-|<0.6$. Adopting $|\delta_-|<0.6$ and the theoretical prejudice that $\delta_+\cong0$, the experimental lifetimes for the $\frac{1}{2}^-$ and $\frac{1}{2}^+$ levels then yield

$$|P_\gamma\ (2.789\ \text{MeV})|=(10.5^{+0.7}_{-2.8}\times10^{-2}/\text{eV})\,|\langle\tfrac{1}{2}^+\tfrac{1}{2}\,|\,V_{\text{PNC}}\,|\,\tfrac{1}{2}^-\tfrac{1}{2}\rangle|\ . \tag{16}$$

The two-body PNC *NN* potential referred to in Eqs. (13)–(16) is assumed to arise from single π, ρ, and ω exchange and has the form[44]

$$V_{\text{PNC}}(r)=\frac{iF_\pi}{M}(\vec\tau_1\times\vec\tau_2)_Z[\vec\sigma(1)+\vec\sigma(2)]\cdot\vec u_\pi(r)$$
$$+\frac{1}{M}\left[\left\{F_0\vec\tau(1)\cdot\vec\tau(2)+\frac{F_1}{2}[\vec\tau(1)+\vec\tau(2)]_Z+\frac{F_2}{2\sqrt6}[3\tau(1)_Z\tau(2)_Z-\vec\tau(1)\cdot\vec\tau(2)]\right\}\right.$$

$$\times\{(1+\mu_v)i[\vec{\sigma}(1)\times\vec{\sigma}(2)]\cdot\vec{u}_\rho(r)+[\vec{\sigma}(1)-\vec{\sigma}(2)]\cdot\vec{v}_\rho(r)\}$$

$$+\left[G_0+\frac{G_1}{2}[\vec{\tau}(1)+\vec{\tau}(2)]_Z\right]\{(1+\mu_s)i[\vec{\sigma}(1)\times\vec{\sigma}(2)]\cdot\vec{u}_\rho(r)+[\vec{\sigma}(1)-\vec{\sigma}(2)]\cdot\vec{v}_\rho(r)\}$$

$$+\frac{K_1}{2}[\vec{\tau}(1)-\vec{\tau}(2)]_Z[\vec{\sigma}(1)+\vec{\sigma}(2)]\cdot\vec{v}_\rho(r)$$

$$+H_1 i[\vec{\tau}(1)\times\vec{\tau}(2)]_Z[\vec{\sigma}(1)+\vec{\sigma}(2)]\cdot\vec{u}_\rho(r)\Big], \tag{17}$$

where

$$r=|\vec{r}_1-\vec{r}_2|\ ,\quad \vec{u}=\left[\vec{p},\frac{e^{-mr}}{4\pi r}\right]\ ,\quad \vec{v}=\left[\vec{p},\frac{e^{-mr}}{4\pi r}\right]\ ,\quad \vec{p}=\vec{p}_1-\vec{p}_2\ ,\quad \mu_v=3.70\ ,\quad \text{and } \mu_s=-0.12\ .$$

(Note that a relative momentum equal to $\vec{p}/2$ appears frequently in the literature.) The coefficients in this meson exchange potential are independent apart from the constraint $K_1=G_1-F_1$. In Table IV these coefficients are given in terms of the underlying strong and PNC weak meson-nucleon couplings. Because of strong interaction corrections, the determination of these couplings for a model of the weak interactions between quarks is a complicated task. One recent quark model calculation[15] using the standard model of Glashow, Weinberg, and Salam yielded the "best values" and "reasonable ranges" shown in Table IV. Ultimately one hopes to deduce the values of these couplings directly from parity nonconservation experiments in few-nucleon and nuclear systems.

C. Shell model calculations of first-forbidden β-decay rates in ^{18}Ne and ^{19}Ne

Four sets of shell model wave functions were employed in calculations of first-forbidden β decay and parity mixing in $A=18$, 19, and 21. In two, denoted by $0+1\ \hbar\omega$-c.m. and $0+1\hbar\omega$-Kuo, the positive and negative shell model bases consist of all possible $0\hbar\omega$ and $1\hbar\omega$ harmonic oscillator configurations. This choice permits an exact projection of the spurious center-of-mass motion that arises in independent-particle shell models, but at the cost of omitting all multiparticle-hole configurations. The effective interaction for the $2s\,1d$ shell is taken from Kuo and Brown,[48] while the cross-shell $1p$-$2s\,1d$ matrix elements are calculated from the Millener-Kurath potential.[49] In the $0+1\hbar\omega$-c.m. calculation the $1f2p$-shell configurations are included only to the extent required for spuriousity projection, while in the $0+1\hbar\omega$-Kuo calculation the $1f2p$ shell interacts via the bare Kuo g matrix.[51] The third calculation, denoted *Z-pds*, employs the potential and single particle energies of Ref. 50. The $1s_{1/2}$-$1p_{3/2}$ core is inert, and all configurations of the valence nucleons in the limited model space $1p_{1/2}$-$2s_{1/2}$-$1d_{5/2}$ are allowed. Thus some multiparticle-hole correlations are included but no projection of spurious components is possible. The final set of wave functions, labeled $1+2\hbar\omega$, was generated by extending the $0+1\hbar\omega$-Kuo calculation to include the $2\hbar\omega$ configurations. This "completes" the shell model space in the sense that the axial charge operator acting on the dominant $0\hbar\omega$ (positive parity) and $1\hbar\omega$ (negative parity) components of wave functions can generate no configuration outside the $1+2\hbar\omega$ basis. In this calculation, the $3s\,2d\,1g$ shell is allowed to interact only through the center-of-mass operator while the $1p$ shell Cohen and Kurath[51] (8—16) and bare Kuo interactions are employed in cases not pre-

TABLE III. β^+ intensities in the decay of ^{19}Ne.

E_x	BR	$f(E)$	logft
0	0.9999	99.57 ±0.12	3.237±0.002
110	$(1.2\pm0.2)\times10^{-4}$	79.78 ±0.10	7.061±0.072
1554	$(2.22\pm0.21)\times10^{-5}$[a]	0.6420±0.0024	5.700±0.041

[a]Combining our BR with that in Ref. 31.

TABLE IV. Weak coupling constants as determined from the "best-value" and "reasonable range" results of Ref. 15 for the Weinberg-Salam model. We take $g_{\pi NN}=13.45$, $g_p=2.79$, $g_\omega=8.37$, and $K_1=G_1-F_1$.

Coefficient	Ref. 6 equivalent	"Best value" (10^{-6})	"Reasonable range" (10^{-6})
F_π	$g_{\pi NN}f_\pi/\sqrt{32}$	1.08	0 :2.71
F_0	$-g_\rho h_\rho^0/2$	1.59	−1.59:4.29
F_1	$-g_\rho h_\rho^1/2$	0.027	0 :0.053
F_2	$-g_\rho h_\rho^2/2$	1.33	1.06:1.54
G_0	$-g_\omega h_\omega^0/2$	0.80	−2.39:4.29
G_1	$-g_\omega h_\omega^1/2$	0.48	0.32:0.80
H_1	$-g_\rho h'^1_\rho/4$	0.0	

viously specified. This calculation requires so much computer time that it was performed only for the 0^+1 ^{18}Ne ground state. In the $0+1h\omega$-c.m., $0+1h\omega$-Kuo, and $1+2h\omega$ calculations the single particle energies were adjusted to optimize the fit to the low-lying levels in ^{18}F, ^{19}F, and ^{21}Ne.

In calculations of two-body operators such as $M^5_{00(2)}$ some correction for the absence of two-nucleon correlations in the independent shell model must be made. This was done by multiplying the two-particle densities by the Miller-Spencer correlation function

$$f(r)=1-\exp(-ar^2)(1-br^2)\ ,$$

with $a=1.1$ fm^{-2} and $b=0.68$ fm^{-2}.[55] This simple function has been shown to reproduce nicely the results obtained with more sophisticated treatments of correlations in PNC matrix elements.[14]

The predicted forbidden β-decay rates of ^{18}Ne and ^{19}Ne are shown in Table V. The exchange current contributions are large, increasing the theoretical rates by a factor of two or more. The momentum-dependent $\Delta J=1$ multipole contributions to the ^{19}Ne transition, with the vector contributions determined by CVC, are totally negligible, in all cases affecting rates at the level of $\lesssim 0.4\%$. Thus the ^{18}Ne and ^{19}Ne transitions are truly analogous, each depending only on the matrix elements of $\hat{M}^5_{00}$ and $\hat{L}^5_{00}$. (Although the latter vanishes in the long wavelength limit, it nevertheless makes a noticeable contribution to the rates, as can be seen from the $q=0$ one-body results.)

The most striking feature of Table V is that, with the exception of the $1+2h\omega$ calculation, the various structure treatments overestimate the PNC doublet β-decay rates by roughly an order of magnitude. This is not entirely surprising. Previous work has demonstrated the importance of 4p2h admixtures ($\cong 25\%$) in the 0^+1 level of ^{18}F: "α-particle" configurations in the $2s\,1d$ shell are energetically favorable, as is apparent from the binding energy of ^{20}Ne. Furthermore, as we mentioned above, operators involving $\vec{p}(i)/M$ strongly couple these $2h\omega$ configurations to the $1h\omega$ basis from which the negative parity state is constructed. The role of $2h\omega$ configurations in reducing matrix elements of the axial charge is also understood: in the long wavelength limit $\langle \hat{M}^5_{00(1)} \rangle$ depends on the one-body density matrix only through the combinations $\psi^-_{\alpha\beta}\equiv\psi_{\alpha\beta}-\psi_{\beta\alpha}$. In the $0+1h\omega$ treatments, the only $\psi_{\alpha\beta}$ that arise are $\psi_{2s_{1/2}1p_{1/2}}$ and $\psi_{1d_{3/2}1p_{3/2}}$, so $\psi^-_{\alpha\beta}=\psi_{\alpha\beta}$. The $2h\omega$ correlations in the 0^+1 state introduce $\psi_{\beta\alpha}$, such as

TABLE V. PNC analog β-decay rates in units of 10^{-6}/sec for various shell model calculations. The one-body and one-body-plus-exchange-current results are ω_1 and ω_{1+2}, while ω_1 ($q=0$) denotes the one-body result with no q-dependent corrections. See Eq. (18) for the definition of α.

Transition	Calculation	ω_{1+2}	ω_1	ω_1 ($q=0$)	α	ω^{exp}
$^{18}\text{Ne}\rightarrow{}^{18}\text{F}(0^-)$	Z-pds	52.2	23.0	14.0	0.65	
	$0+1h\omega$-Kuo	75.3	29.5	26.2	0.63	8.6±1.2
	$1+2h\omega$	4.80	1.84	1.00	0.83	
$^{19}\text{Ne}\rightarrow{}^{19}\text{F}(\frac{1}{2}^-)$	Z-pds	104.0	50.2	42.4	0.48	
	$0+1h\omega$-c.m.	53.4	23.8	21.3	0.53	4.8±0.8
	$0+1h\omega$-Kuo	41.3	17.1	15.3	0.58	

$\psi_{1p_{1/2}2s_{1/2}}$, that, for an attractive NN potential, are expected to have the same sign as the $\psi_{\alpha\beta}$, thereby reducing $\psi^{-}_{\alpha\beta}$.[52] Similar conclusions on the importance of $2h\omega$ configurations have emerged from recent calculations of the $0^+ \leftrightarrow 0^-$ β-decay and μ-capture transition rates in mass 16.[53]

One feature of the results in Table V has important implications for calculations of parity mixing matrix elements. Although the various structure assumptions produce ^{18}Ne $0^+ \rightarrow 0^-$ β-decay rates that differ by as much as a factor of 16, the calculations are consistent in their predictions of the strength of the exchange current *relative* to the one-body amplitude. The ^{18}F calculations all satisfy

$$\frac{\langle 0^-0||\hat{M}^{5}_{0(2)}||0^+1\rangle}{\langle 0^-0||\hat{M}^{5}_{0(1)}(q=0)||0^+1\rangle}\equiv\alpha=0.73\pm0.10\ , \tag{18}$$

where $M^{5}_{00(1)}$ $(q=0)$ is the long-wavelength limit of the one-body axial charge operator. This very weak dependence of α on nuclear models will allow us (in Sec. III D) to use measured β-decay rates to remove most of the nuclear structure dependence from predictions of PNC mixing matrix elements.

Since the ^{19}Ne β decay is also dominated by the axial charge operator, we can repeat this analysis. We find

$$\frac{\langle \frac{1}{2}^+\frac{1}{2}||\hat{M}^{5}_{0(2)}||\frac{1}{2}^-\frac{1}{2}\rangle}{\langle \frac{1}{2}^+\frac{1}{2}||\hat{M}^{5}_{0(1)}(q=0)||\frac{1}{2}^-\frac{1}{2}\rangle}=0.53\pm0.05 \tag{19}$$

for the Z-pds, $0+1h\omega$-c.m., and $0+1h\omega$-Kuo wave functions. So again a scaling of one- and two-body amplitudes persists among calculations that differ significantly (by a factor of 2.5) in predicting absolute β-decay rates. The difficult $1+2h\omega$ calculation was not attempted for ^{19}Ne, and all of the available wave functions overestimate the experimental rate,

$$\omega=(4.8\pm0.8)10^{-6}/\text{sec}\ ,$$

by a factor of 8 or more. In particular, the suppression factor $\beta=(\omega^{\text{exp}}/\omega^{\text{th}})^{1/2}$ is 0.34 ± 0.03 for the $A=19$ $0+1h\omega$-Kuo calculation, nearly the same value (0.33 ± 0.03) found for the corresponding wave functions for $A=18$. In $A=18$ we demonstrated that this suppression could be attributed to $2h\omega$ excitations. It is reasonable to assume that the suppression in $A=19$ has the same origin.

The origin of relations (18) and (19) is familiar in a different context, that of representing two-body PNC potentials by equivalent one-body operators.[54] The PNC potential (or exchange current operator) consists of two sets of terms: true two-body components where the quantum numbers of pairs of nucleons are changed, and components that are semidiagonal in one quantum number. The latter, representing the interaction of valence nucleons with an inert core, are usually the dominant contribution to the nuclear matrix element. These semidiagonal terms can be exactly represented by an equivalent one-body operator. In a Fermi gas model with $Z=N$ the effective one-body exchange current operator $\hat{M}^{5}_{00\,\text{eff}}$ is

$$\begin{aligned}\langle \vec{k}_1\lambda_1\rho_1|\hat{M}^{5}_{00\,\text{eff}}|\vec{k}_2\lambda_2\rho_2\rangle=&\sum_{\vec{k}'\lambda'\rho'}^{k_f}(\langle \vec{k}_1\lambda_1\rho_1\vec{k}'\lambda'\rho'|\hat{M}^{5}_{00(2)}|\vec{k}_2\lambda_2\rho_2\vec{k}'\lambda'\rho'\rangle\\&-\langle \vec{k}_1\lambda_1\rho_1\vec{k}'\lambda'\rho'|\hat{M}^{5}_{00(2)}|\vec{k}'\lambda'\rho'\vec{k}_2\lambda_2\rho_2\rangle)\\=&\frac{1}{\sqrt{4\pi}}\frac{g^2}{4\pi^3M^2F_A}\langle\rho_1|\tau_+|\rho_2\rangle\delta(\vec{k}_1-\vec{k}_2)\sum_{\vec{k}'}\left\langle\lambda_1\left|\frac{\sigma\cdot(\vec{k}_1-\vec{k}')}{(\vec{k}_1-\vec{k}')^2+m_\pi{}^2}\right|\lambda_2\right\rangle\\=&\frac{1}{\sqrt{4\pi}}\frac{g^2\rho_A W_{k_F}(\tilde{k}_1,\tilde{m}_\pi)}{2m_\pi{}^2MF_A{}^2}\left\langle\vec{k}_1\lambda_1\rho_1\left|F_A\tau_+\frac{\vec{\sigma}\cdot\vec{k}_1}{M}\right|\vec{k}_2\lambda_2\rho_2\right\rangle\end{aligned} \tag{20}$$

with the nuclear density ρ_A given in terms of the Fermi momentum k_F by $\rho_A=2k_F{}^3/3\pi^2$, $\tilde{k}_1=|\vec{k}_1|/k_F$, and $\tilde{m}_\pi=m_\pi/k_F$. Only the exchange term contributes to the sum. The function W_{k_F} is given in the independent particle limit by

$$\begin{aligned}W_{k_F}(\tilde{m}_\pi,\tilde{k}_1)=&\frac{3\tilde{m}_\pi{}^2}{32\tilde{k}_1{}^3}4\tilde{k}_1(1+\tilde{k}_1{}^2+\tilde{m}_\pi{}^2)-[(1-\tilde{k}_1{}^2)^2+2\tilde{m}_\pi{}^2(1+\tilde{k}_1{}^2)+\tilde{m}_\pi{}^4]\ln\left[\frac{\tilde{m}_\pi{}^2+(1+\tilde{k}_1)^2}{\tilde{m}_\pi{}^2+(1-\tilde{k}_1)^2}\right]\\&\rightarrow 1\ \text{ as }\tilde{m}_\pi\rightarrow\infty\ .\end{aligned} \tag{21}$$

Thus we see that, in a Fermi gas model, $\hat{M}^{5}_{00\,\mathrm{eff}}$ is precisely $\hat{M}^{5}_{00(1)}$ $(q=0)$ multiplied by a scale function α,

$$\alpha=\frac{g^2\rho_A W_{k_F}(\tilde{k}_1,\tilde{m}_\pi)}{2m_\pi{}^2MF_A{}^2}\ . \tag{22}$$

Although W_{k_F} is sensitive to the mass of the exchanged particle, it is relatively insensitive to $\tilde{k}_1$, varying smoothly from 0.20 to 0.14 over the range $0<\tilde{k}_1<1$ for $m_\pi=140$ MeV. Thus to a good approximation we can replace W_{k_F} by an average value $\langle W_{k_F}\rangle\sim 0.17$. For a nuclear matter density of $\rho_A=0.195$ nucleons/fm^3, we then find a scale *factor* $\alpha=0.84$ which then gives the strength of the many-body matrix elements of $\hat{M}^{5}_{00(2)}$ relative to those for $\hat{M}^{5}_{00(1)}$ $(q=0)$. Inclusion of a correlation function in the two-particle density distributions will affect this value somewhat. In our shell model calculations for ^{18}F and ^{19}F the Miller-Spencer correlation function[55] reduced the $\Delta I=1$ pion-exchange matrix elements to 0.74 ± 0.03 of their uncorrelated values. Thus a more correct estimate of α is

$$\alpha^{\mathrm{cor}}\sim(0.84)(0.74)\sim 0.62$$

a value close to the empirical scaling factors deduced above from full two-body shell model calculations in $A=18$ and 19.

D. Constraints on F_π from first-forbidden β decay

A comparison of Eqs. (5), (12), and (17) reveals that the $\Delta I=1$ pion-exchange contribution to the nuclear PNC Hamiltonian

$$V^{\pi}_{\mathrm{PNC}}=\tfrac{1}{2}\sum_{\substack{ij\\ i\neq j}}\left[-\frac{F_\pi m_\pi{}^2}{2\pi M}\right][\vec{\tau}(i)\times\vec{\tau}(j)]_{10}[\vec{\sigma}(i)+\vec{\sigma}(j)]\cdot\hat{r}_{ij}\phi(m_\pi r_{ij}) \tag{23a}$$

is proportional to the two-body contribution to $\hat{M}^{5}_{00}$,

$$\hat{M}^{5}_{00(2)}=\tfrac{1}{2}\sum_{\substack{ij\\ i\neq j}}\left[\pm\frac{F_1^V g_{\pi NN}{}^2 m_\pi{}^2}{16\sqrt{2}\pi^{3/2}F_A M^2}\right][\vec{\tau}(i)\times\vec{\tau}(j)]_{1\pm1}[\vec{\sigma}(i)+\vec{\sigma}(j)]\cdot\hat{r}_{ij}\phi(m_\pi r_{ij}) \tag{23b}$$

apart from a rotation in isospin, as shown schematically in Fig. 10, Eqs. (23) have been written in terms of spherical isospin components:

$$\vec{\mathrm{A}}_{10}\equiv A_Z\ ,$$

$$\vec{\mathrm{A}}_{1\pm1}=\mp\frac{1}{\sqrt{2}}(A_x\pm iA_y)\ .$$

Our β-decay measurements determine, effectively, the matrix elements of $\hat{M}^{5}_{00}=\hat{M}^{5}_{00(1)}+\hat{M}^{5}_{00(2)}$. The scaling relations, Eqs. (18) and (19), allow us to place stringent and *largely model independent* constraints on the matrix elements of $\hat{M}^{5}_{00(2)}$ and thus, assuming nuclear states of good isospin and using Eqs. (23), on the strength of the pion-exchange contribution to the $\Delta I=1$ PNC mixing matrix elements. In the case of ^{18}F we find in the long wavelength approximation

$$\langle 0^-0\,|\,V^{\pi}_{\mathrm{PNC}}\,|\,0^+1\rangle\cong(0.366\pm0.055\ \mathrm{MeV})F_\pi\ .$$

The forbidden contributions to the β-decay amplitude are not completely negligible, owing to the structure suppression of the matrix elements of M^{5}_{00} $(q=0)$. However, because of the time reversal properties of $\hat{L}^{5}_{00}$, the $O(q)$ corrections depend on the density matrix element combinations $\psi^{+}_{\alpha\beta}\equiv\psi_{\alpha\beta}+\psi_{\beta\alpha}$, which are enhanced by the multiparticle-hole correlations. Thus the $O(q)$ corrections are not subject to the delicate cancellations occurring for $\langle\hat{M}^{5}_{00}\ (q\to0)\rangle$ and should be more reliably predicted by the shell model. Indeed, our various calculations yield quite consistent predictions of these $O(q)$ corrections, e.g.,

$$\langle 0^-0\,|\,V^{\pi}_{\mathrm{PNC}}\,|\,0^+1\rangle=\begin{cases}(0.326\pm0.051\ \mathrm{MeV})F_\pi,\ 0+1h\omega\text{-Kuo}\ ,\\ (0.322\pm0.051\ \mathrm{MeV})F_\pi,\ 1+2h\omega\end{cases}$$

and we accept as our final result

$$\langle 0^-0 \,|\, V_{\rm PNC}^{\pi} \,|\, 0^+1 \rangle = (0.324 \pm 0.053 \text{ MeV}) F_\pi \ . \tag{24}$$

The PNC matrix element in ^{18}F also involves heavy meson contributions. We argue in the next section that these terms are small, possibly on the order of 5% of $\langle 0^-0 \,|\, V_{\rm PNC}^{\pi} \,|\, 0^+1 \rangle$, and add constructively. Therefore we ignore these contributions and derive a conservative upper limit on F_π from the experimental circular polarization,

$$P_\gamma = (-0.8 \pm 1.2) \times 10^{-3} \ .$$

Using the bounds on $\langle V_{\rm PNC}^{\pi} \rangle$ above and on the ratio

$$|\langle T_1^{\rm mag;\gamma} \rangle / \langle T_1^{\rm el;\gamma} \rangle|$$

appearing in Eq. (13), we find

$$|P_\gamma| = (1.83 \pm 0.43) \times 10^3 F_\pi \tag{25}$$

so that $|F_\pi| \leq 1.4 \times 10^{-6}$, or equivalently $|f_\pi| \leq 0.59 \times 10^{-6}$. This upper bound on F_π is essentially independent of nuclear structure assumptions. The recent quark model estimates of Desplanques, Donoghue, and Holstein [15](DDH) defined a broad "reasonable range" of $0 < F_\pi < 2.73 \times 10^{-6}$ ($0 < f_\pi < 1.14 \times 10^{-6}$) and a "best value" of $F_\pi \sim 1.09 \times 10^{-6}$ ($f_\pi \sim 0.46 \times 10^{-6}$) in the Glashow-Weinberg-Salam model. Our ^{18}Ne β-decay measurement, when combined with the upper limit on P_γ, excludes a considerable fraction of the "reasonable range" for F_π. The DDH "best value" prediction for $|P_\gamma|$, using the value for $\langle V_{\rm PNC}^{\pi} \rangle$ given in Eq. (24), is $(2.00 \pm 0.49) \times 10^{-3}$. An experiment currently underway[56] should attain this sensitivity, so we may soon have firm knowledge of the strength of F_π.

E. Shell model predictions of parity mixing, γ decays, and Gamow-Teller strengths in ^{18}F, ^{19}F, and ^{21}Ne

In most cases the connection between the underlying weak meson-nucleon couplings and nuclear PNC observables can only be made through nuclear structure calculations. While the shell model bases for light nuclei such as ^{18}F, ^{19}F, and ^{21}Ne are tractable, realistic structure calculations for heavier nuclei are often prohibitively difficult. Therefore we anticipate that careful attention to the structure of these light nuclei will provide some of the most reliable nuclear constraints on the parameters of the PNC *NN* potential.

In Table VI matrix elements of the nuclear operators appearing in the PNC potential of Eq (17) are given for the ^{18}F, ^{19}F, and ^{21}Ne wave functions described earlier. One striking feature of these results is the uniform relative strength of the terms comprising the mixing matrix elements, despite the large differences in absolute strengths in various calculations. This justifies our neglect in the previous section of the $\Delta I = 1$ heavy meson contributions to the ^{18}F matrix element: with the DDH "best value" couplings, these terms enhance the matrix elements by only $\sim 5\%$ in *each* of the four calculations. Even more significant is the illustration, in the last column in Table VI, that for both ^{19}F and ^{21}Ne the

TABLE VI. Shell model predictions of the matrix elements for the nuclear operators appearing in Eq. (18), in MeV. Folding these with the DDH "best value" couplings of Table IV gives the mixing matrix elements (in eV) and the isovector/isoscalar ratios shown in the last two columns.

	Calculation	F_π	F_0	F_1	G_0	G_1	K_1	H_1	$\langle V_{\rm PNC}^{\rm DDH} \rangle_{\rm best}$	$\frac{\langle \Delta I=0 \rangle}{\langle \Delta I=1 \rangle_{\rm DDH}}$
^{18}F:	$-i\langle 0^-0 \,\|\, V_{\rm PNC} \,\|\, 0^+1 \rangle$									
	Z-pds	0.722		0.107		0.034	0.019	0.048	0.81	
	$0+1h\omega$-c.m.	1.175		0.232		0.074	0.038	0.085	1.33	
	$0+1h\omega$-Kuo	0.953		0.190		0.060	0.030	0.069	1.08	
	$1+2h\omega$	0.247		0.056		0.018	0.009	0.020	0.28	
^{19}F:	$-i\langle \frac{1}{2}^-\frac{1}{2} \,\|\, V_{\rm PNC} \,\|\, \frac{1}{2}^+\frac{1}{2} \rangle$									
	Z-pds	0.825	0.415	0.189	0.085	0.059	0.027	0.062	1.67	0.77
	$0+1h\omega$-c.m.	0.643	0.397	0.143	0.074	0.045	0.022	0.051	1.42	0.95
	$0+1h\omega$-Kuo	0.606	0.373	0.133	0.070	0.042	0.021	0.048	1.34	0.92
^{21}Ne:	$-i\langle \frac{1}{2}^-\frac{1}{2} \,\|\, V_{\rm PNC} \,\|\, \frac{1}{2}^+\frac{1}{2} \rangle$									
	$0+1h\omega$-c.m.	0.377	−0.258	0.085	−0.051	0.026	0.011	0.027	−0.022	−1.05
	$0+1h\omega$-Kuo	0.344	−0.234	0.076	−0.046	0.023	0.009	0.024	−0.018	−1.06

predicted relative sizes of the $\Delta I=0$ and $\Delta I=0$ PNC matrix elements are very insensitive to the nuclear structure model. This suggests that the ^{19}Ne forbidden β-decay measurement may provide an important constraint on the ^{19}F PNC matrix element despite the presence of strong $\Delta I=0$ contributions. We assume that a "correct" shell model calculation will reproduce the ^{19}Ne β-decay rate but will not significantly change the *relative* strengths of the various nuclear matrix elements involved in the β decay and parity mixing. If we scale the matrix elements to reproduce the measured ^{19}Ne β-decay rate, we find that the DDH couplings then predict a PNC matrix element of

$$|\langle|V_{\rm PNC}|\rangle|=0.46\pm0.08 \text{ eV}$$

and

$$A_\gamma=(-8.9\pm1.6)\times10^{-5},$$

in good agreement with the experimental result

$$A_\gamma=(-7.1\pm2.1)\times10^{-5}.$$

Thus the DDH "best values" for F_π and F_0 appear very reasonable. (These couplings effectively determine the ^{18}F and ^{19}F matrix elements unless the DDH broad "reasonable ranges" for other couplings prove too conservative, a possibility that cannot currently be ruled out.)

The parity mixing in ^{21}Ne fits nicely into this picture. The experimental result

$$P_\gamma=(0.8\pm1.4)\cdot10^{-3}$$

requires

$$|\langle V_{\rm PNC}|\rangle|\leq0.029 \text{ eV},$$

a small value in comparison to our ^{18}F and ^{19}F results. Our calculations using DDH couplings yield $|\langle|V_{\rm PNC}|\rangle|=0.018$ and 0.022 eV; the consistency with experiment is due to the nearly exact cancellation between the F_π and F_0 contributions, e.g., 0.373 and -0.372 eV in the $0+1\hbar\omega$-Kuo calculation. The experimental constraint on $|\langle|V_{\rm PNC}|\rangle|$ is so severe that, even if an uncertainty of a factor of 3 is introduced in the overall normalization of the calculated nuclear matrix elements, one finds $F_\pi/F_0\sim(F_\pi/F_0)_{\rm DDH}$. This result, however, is sensitive to our approximate treatment of correlations, which affect the relative contributions of the pion and heavy meson matrix elements significantly.

In Tables VII–IX we compare the electromagnetic properties of the low-lying levels in ^{18}F, ^{19}F/^{19}Ne, and ^{21}Ne/^{21}Na with shell model predictions using what we believe are the best of the wave functions discussed above ($0+1\hbar\omega$-Kuo, and $1+2\hbar\omega$ for the ^{18}F 0^+1 state). A similar comparison was made by Millener *et al.* for ^{21}Ne,[13] with results quite similar

TABLE VII. Reduced transition strengths for γ-ray transitions between low-lying ($E_x\leq4$ MeV) states in ^{18}F calculated with $0+1\hbar\omega$-Kuo wave functions. [We exclude isoscalar $E1$ transitions and transitions involving states with large 4p2h components (see text). Calculations performed with an oscillator parameter $b=1.75$ fm and with the effective charges of Ref. 13.]

$E_i\rightarrow E_f$ (MeV)	$J_i^\pi\rightarrow J_f^\pi$	Multipole	$B^{\rm exp}$ (W.u.)	$B^{\rm th}$ (W.u.)
0.94 → 0.00	$3^+\rightarrow1^+$	$E2$	5.8 ±0.2[a]	7.1
1.04 → 0.00	$0^+;1\rightarrow1^+;0$	$M1$	10.3 ±1.5[a]	9.4
1.12 → 0.94	$5^+\rightarrow3^+$	$E2$	6.50±0.22[a]	6.5
2.10 → 1.08	$2^-\rightarrow0^-$	$E2$	15 ±2[d]	12
3.06 → 0.00	$2^+;1\rightarrow1^+;0$	$M1$	>0.2[d]	0.08
→ 0.94	$\rightarrow3^+$	$M1$	>2.1[d]	3.8
→ 1.04	$\rightarrow0^+;1$	$E2$	>5.6[d]	5.4
3.13 → 1.04	$1^-\rightarrow0^+;1$	$E1$	$(1.3\pm0.1)\times10^{-4}$[d]	28×10^{-4}[b]; 7.0×10^{-4}[c]
→ 1.08	$\rightarrow0^-$	$M1$	$(2.3\pm0.2)\times10^{-3}$[d]	10×10^{-3}
3.72 → 0.00	$1^+\rightarrow1^+$	$M1$	$>3\times10^{-3}$[d]	0.7×10^{-5}
→ 1.04	$\rightarrow0^+;1$	$M1$	>0.14[d]	0.28
→ 3.06	$\rightarrow2^+;1$	$M1$	>0.2[d]	1.01
3.79 → 2.10	$3^-\rightarrow2^-$	$M1$	$(2.1\pm0.2)\times10^{-3}$[d]	11×10^{-3}
		$E2$	$(3.4\pm1.9)\times10^{-1}$[d]	0.3×10^{-1}
3.06	$\rightarrow2^+;1$	$E1$	$(5.0\pm1.1)\times10^{-3}$[a]	2.4×10^{-3}

[a]Taken from F. Ajzenberg-Selove, Nucl. Phys. A392, 1 (1983).
[b]$0\hbar\omega$ wave function for $0^+;1$ state.
[c]$2\hbar\omega$ wave function for $0^+;1$ state.
[d]G. C. Ball *et al.*, Nucl. Phys. A386, 333 (1982).

TABLE VIII. Reduced transition strengths for γ-ray transitions between low-lying ($E_x \leq 4$ MeV) states in ^{19}F and ^{19}Ne calculated with $0+1\hbar\omega$-Kuo wave functions. (Calculated with an oscillator parameter $b = 1.75$ fm and with the effective charges of Ref. 13. Transitions from the $\frac{3}{2}^+$ 3.91 MeV state in ^{19}F are omitted since this state is not generated in $0\hbar\omega$ calculations.)

		^{19}F			^{19}Ne		
$J_i^\pi \rightarrow J_f^\pi$	Multipole	$E_i \rightarrow E_f$ (MeV)	B^{exp} (W.u.)[a]	B^{th} (W.u.)	$E_i \rightarrow E_f$ (MeV)	B^{exp} (W.u.)[a]	B^{th} (W.u.)
$\frac{1}{2}^- \rightarrow \frac{1}{2}^+$	$E1$	0.11 → 0.0	$(1.2 \pm 0.1)\times 10^{-3}$	3.5×10^{-3}	0.28 → 0.0	$(1.06\pm 0.05)\times 10^{-3}$	3.5×10^{-3}
$\frac{5}{2}^+ \rightarrow \frac{1}{2}^+$	$E2$	0.20 → 0.0	6.95 ± 0.08	7.6	0.24 → 0.0	13.2 ± 0.5	14
$\frac{5}{2}^- \rightarrow \frac{1}{2}^-$	$E2$	1.35 → 0.11	20 ± 3	21	1.51 → 0.28	58 ± 20	20
$\rightarrow \frac{5}{2}^+$	$E1$	→ 0.20	$(6.5 \pm 2.2)\times 10^{-6}$	8.0×10^{-6}	→ 0.24	$(5.7 \pm 2.5)\times 10^{-5}$	0.80×10^{-5}
$\frac{3}{2}^- \rightarrow \frac{1}{2}^+$	$E1$	1.46 → 0.0	$(1.0 \pm 0.2)\times 10^{-3}$	5.4×10^{-3}	1.62 → 0.0	$(4.5 \pm 1.4)\times 10^{-4}$	5.4×10^{-4}
$\rightarrow \frac{1}{2}^-$	$M1$	→ 0.11	$(9.1 \pm 1.9)\times 10^{-2}$	12×10^{-2}	→ 0.28	$(6.3 \pm 1.6)\times 10^{-2}$	8.3×10^{-2}
	$E2$		25 ± 11	23			21
$\rightarrow \frac{5}{2}^+$	$E1$	→ 0.20	$(8.1 \pm 1.9)\times 10^{-4}$	39×10^{-4}	→ 0.24	$(3.6 \pm 1.4)\times 10^{-4}$	39×10^{-4}
$\frac{3}{2}^+ \rightarrow \frac{1}{2}^+$	$M1$	1.55 → 0.0	$(4.3 \pm 2.5)\times 10^{-2}$	0.35×10^{-2}	1.54 → 0.0		2.8×10^{-3}
$\rightarrow \frac{1}{2}^-$	$E1$	→ 0.11	$(4.4 \pm 2.6)\times 10^{-3}$	5.2×10^{-3}	→ 0.28	$(1.0 \pm 0.7)\times 10^{-3}$	5.2×10^{-3}
$\rightarrow \frac{5}{2}^+$	$M1$	→ 0.20	2.3 ± 1.4	2.2	→ 0.24	0.50 ± 0.28	1.6
$\frac{9}{2}^+ \rightarrow \frac{5}{2}^+$	$E2$	2.78 → 0.20	8.2 ± 0.9	7.7	2.79 → 0.24	17 ± 4	17
$\frac{7}{2}^- \rightarrow \frac{5}{2}^+$	$E1$	4.00 → 0.20	$(2.3 \pm 1.0)\times 10^{-4}$	57×10^{-4}			57×10^{-4}
$\rightarrow \frac{5}{2}^-$	$M1$	→ 1.35	$(6.2 \pm 2.4)\times 10^{-2}$	13×10^{-2}			9.6×10^{-2}
$\rightarrow \frac{3}{2}^-$	$E2$	→ 1.46	49 ± 30	18			16

[a]F. Ajzenberg-Selove, Nucl. Phys. A392, 1 (1983).

TABLE IX. Reduced transition strengths for γ-ray transitions between low-lying ($E_x \leq 4$ MeV) states in ^{21}Ne and ^{21}Na calculated with $0+1\hbar\omega$-Kuo wave functions. (Calculated with an oscillator parameter $b = 1.75$ fm and with the effective charges of Ref. 13. Wave functions for negative parity states other than the $\frac{1}{2}^-$ were not calculated.)

		^{21}Ne			^{21}Na		
$J_i^\pi \to J_f^\pi$	Multipole	$E_i \to E_f$ (MeV)	B^{exp} (W.u.)[a]	B^{th} (W.u.)	$E_i \to E_f$ (MeV)	B^{exp} (W.u.)[a]	B^{th} (W.u.)
$\frac{5}{2}^+ \to \frac{3}{2}^+$	$M1$	0.35 → 0.0	$(7.2 \pm 0.2)\times 10^{-2}$	7.7×10^{-2}	0.33 → 0.0	$(8.5 \pm 0.1)\times 10^{-2}$	10.2×10^{-2}
	$E2$		24 ± 3	25		36^{+32}_{-22}	29
$\frac{7}{2}^+ \to \frac{3}{2}^+$	$E2$	1.75 → 0.0	11 ± 4	11	1.72 → 0.0	$5.3^{+4.4}_{-2.6}$	13
$\to \frac{5}{2}^+$	$M1$	→ 0.35	0.14 ± 0.02	0.12	→ 0.33	$0.28^{+0.18}_{-0.08}$	0.16
	$E2$		15 ± 4	19		21^{+30}_{-12}	22
$\frac{1}{2}^- \to \frac{3}{2}^+$	$E1$	2.79 → 0.0	$< 1.3\times 10^{-6}$	91×10^{-6}	2.80 → 0.0	$< 55\times 10^{-6}$	91×10^{-6}
$\to \frac{5}{2}^+$	$M2$	→ 0.35	0.48 ± 0.3	0.53	→ 0.33	< 2.0	0.56
	$E3$		13 ± 6	9.5			11
$\leftrightarrow \frac{1}{2}^+$	$E1$	← 2.80		0.10×10^{-3}	→ 2.42	$(2.2 \pm 0.4)\times 10^{-3}$	0.10×10^{-3}
$\frac{1}{2}^+ \to \frac{3}{2}^+$	$M1$	2.80 → 0.0	$0.15^{+0.10}_{-0.04}$	0.32	2.42 → 0.0	$0.77^{+0.29}_{-0.17}$	0.40
$\to \frac{5}{2}^+$	$E2$	→ 0.35	< 15	0.97	→ 0.33	< 60	0.60
$\frac{9}{2}^+ \to \frac{5}{2}^+$	$E2$	2.87 → 0.35	22 ± 5	15			15
$\to \frac{7}{2}^+$	$M1$	→ 1.75	0.27 ± 0.07	0.19			0.24
	$E2$		10 ± 4	9.9			8.9
$\frac{5}{2}^+ \to \frac{3}{2}^+$	$M1$	3.73 → 0.0	$> 2.5\times 10^{-2}$	15×10^{-2}	3.54 → 0.0		18×10^{-2}
$\to \frac{5}{2}^+$	$M1$	→ 0.35	$> 0.4\times 10^{-2}$	2.2×10^{-2}	→ 0.33		3.3×10^{-2}
$\to \frac{7}{2}^+$	$M1$	→ 1.75	$> 1.4\times 10^{-2}$	29×10^{-2}	→ 1.72		36×10^{-2}

[a]From P. M. Endt and C. Van der Leun, Nucl. Phys. A310, 1 (1978).

TABLE X. Gamow-Teller strengths $|\langle J_f||\sum_{i=1}^{A}\sigma(i)\tau_-(i)||J_i\rangle|$ for shell model $0h\omega$ wave functions.

Transition	Calculation	Experiment
$^{18}\text{Ne}\rightarrow{}^{18}\text{F}(1^+0)$[a]	2.28	1.79±0.01
$^{19}\text{Ne}\rightarrow{}^{19}\text{F}(\frac{1}{2}^+\frac{1}{2})$	1.67	1.82±0.01
$\rightarrow{}^{19}\text{F}(\frac{3}{2}^+\frac{1}{2})$	0.015	0.12±0.01
$^{21}\text{Na}\rightarrow{}^{21}\text{Ne}(\frac{3}{2}^+\frac{1}{2})$	1.06	1.13±0.04
$\rightarrow{}^{21}\text{Ne}(\frac{5}{2}^+\frac{1}{2})$	0.53	0.63±0.02

[a]The 1.70 1^+0 state in ^{18}F is not generated in $0h\omega$ calculations so we omit the transition to this state.

to ours.

The ^{18}F calculations do not quite reproduce the suppression of $1^-0\rightarrow 0^+1$ $E1$ transition although use of the $2h\omega$ positive parity wave function for the 0^+1 state reduces significantly the disagreement with experiment. Unfortunately we could not generate $2h\omega$ wave functions for other states in ^{18}F because of computational limitations. As a result we cannot discuss a number of transitions from positive parity states that clearly have strong $2h\omega$ components. These include the 2^+0 states at 2.52 and 3.84 MeV (the $0h\omega$ calculation generates only a single 2^+0 state at 3.38 MeV) the 3^+0 state at 3.36 MeV (which the $0h\omega$ shell model places at 4.89 MeV) and the 1^+0 4p2h state at 1.70 MeV. The $A=19$ results reproduce experiment well in most cases, although the $\frac{1}{2}^-\rightarrow\frac{1}{2}^+$ and $\frac{3}{2}^-\rightarrow\frac{1}{2}^+$ $B(E1)$ values are a factor of ~ 3 larger than experiment. The $A=21$ calculations in most cases agree with experiment but there are two obvious discrepancies—both $E1$ transitions. The ^{21}Ne $\frac{1}{2}^-\rightarrow\frac{3}{2}^+$ decay is too strong by nearly two orders of magnitude. However, the experimental rate is extraordinarily suppressed ($\sim 1.3\times 10^{-6}$ W.u.), so that qualitatively the theoretical result (9.1×10^{-5} W.u.) is reasonable. The γ-decay rate for the $\frac{1}{2}^-\rightarrow\frac{1}{2}^+$ transition in ^{21}Na, $B(E1)=(2.2\pm 0.4)\times 10^{-3}$ W.u., is underestimated in the calculations by a factor of 20. Again the transition is relatively weak, and on an absolute scale a discrepancy of 2×10^{-3} W.u. is typical of the shell model predictions for other $E1$ transitions in, e.g., ^{19}F. Because this γ-decay transition connects the members of the parity-mixed doublet, any discrepancy is disturbing. However, it is difficult to assess what significance this has for parity mixing since the matrix elements of the $E1$ operator and the scalar PNC operator depend on different sets of density matrix elements.

Finally, for completeness, in Table X we compare calculated Gamow-Teller strengths to those extracted from β-decay ft values. The $2s\,1d$ shell estimates of the strengths are quite reasonable, as we anticipated, since the Gamow-Teller operator cannot couple $0h\omega$ configurations to states outside this basis. For the reasons cited above, the decay to the 1^+0 1.70-MeV state in ^{18}F was not calculated.

From this scant evidence it is difficult to find systematic indications of wave function failures such as we uncovered in our studies of the axial-charge β decays in ^{18}F and ^{19}F. The only obvious failure in the calculations is the prediction of the $E1$ rates. We found in ^{18}F that, as shell model calculations are improved, both the PNC matrix element and the $E1$ transition strength are weakened and approach the experimental results. This and the observation that the discrepancies between experiment and the $0+1h\omega$-Kuo results are comparable in mass 18 and 19 strongly suggest that inclusion of the $2h\omega$ configurations in the ^{19}F calculations must be quite important. Unfortunately no β-decay test of the parity-mixed doublet is possible for ^{21}Ne, and $2h\omega$ calculations for this system are not practical at present.

IV. CONCLUSIONS

The two principal issues we have addressed are the determination of PNC meson-nucleon couplings from parity-mixing light nuclei and an assessment of shell model techniques for calculation of PNC nuclear matrix elements. The β-decay measurements we have reported in ^{18}Ne and ^{19}Ne offer, for the first time, an opportunity to disentangle these issues.

It is probably best to discuss the shell model in the context of other recent work on the question of exchange current amplitudes in nuclei. The axial charge operator is of great interest because the exchange current is of the same order v/c as the one-body current. (This also occurs for the space-like part of the vector current, but there the strong isovector magnetic moment, $\mu_V=4.70$, tends to mask the two-body contributions.) The large exchange-

current enhancements we predict in the ^{18}Ne $0^+ \rightarrow 0^-$ and ^{19}Ne $\frac{1}{2}^+ \rightarrow \frac{1}{2}^-$ β-decay rates are similar to those predicted in

$$^{16}\mathrm{N}(0^-) \rightarrow {}^{16}\mathrm{O}(0^+) + e^+ + \nu_e \ ,$$

$$\mu^- + {}^{16}\mathrm{O}(0^+) \rightarrow {}^{16}\mathrm{N}(0^-) + \nu_\mu \ ,$$

and in the mirror β decays of the $A=12$ triad.[53,57]

Our measured rates for the forbidden β decays of ^{18}Ne and ^{19}Ne are suppressed by a factor of ~ 9 compared to the predictions of the $0h\omega + 1h\omega$ shell model. In $A=18$ we have shown that inclusion of $2h\omega$ configurations reduces the matrix elements of both the one- and two-body axial charge operators by more than a factor of 10, bringing the predictions into reasonable accord with experiment. We expect that neglect of $2h\omega$ configurations may also account for the discrepancy in $A=19$. Related problems are also observed in the $E1$ transitions, with the $E1$ analog of the parity mixing in ^{19}F having a decay rate ~ 3 times slower than the $0h\omega + 1h\omega$ predictions. In $A=18$ the predicted $E1$ rates are reduced when $2h\omega$ configurations are included, bringing the theoretical estimates closer to experiment. The $0h\omega + 1h\omega$ results for the β and γ analogs of the parity mixing in ^{18}F and ^{19}F are shown in Fig. 11.

Independent evidence for the importance of careful nuclear structure treatments in understanding the observed suppression of axial charge transitions has recently been published.[53,58] Towner and Khanna found that inclusion of $2h\omega$ components in the ^{16}O wave function reduced the estimate for the ^{16}N β-decay rate by a factor of 2–3, producing agreement with experiment.[53] Nozawa, Kohyama, and Kubodera found that the exchange current in $A=2$ is reduced significantly when D-wave components induced by the short-range tensor force are included in the deuteron wave function. They speculate that this indicates the need for including high-lying configurations in more complex nuclei.[58] Clearly all of this work reinforces our conclusion that the PNC two-body operators, which are closely related to the axial charge operator, are more difficult to evaluate in the shell model than originally supposed.

Fortunately, in $A=18$ and $A=19$, there is a way to circumvent almost entirely these shell-model difficulties. It relies on three regularities we observe in our calculations.

(1) Although the *absolute* matrix elements of the axial charge are very sensitive to the nuclear structure model, we find that the *relative* contributions of the one- and two-body axial charge operators are remarkably insensitive to the model—a result we explain by reducing the two-body operator to an effective one-body form proportional to the one-body axial charge. This scaling allows us to determine the exchange current matrix element from the β-decay rate. Since the two-body axial charge operator is identical, apart from isospin projection and coupling constants, to the $\Delta I=1$ pion exchange potential, we then know the strength of this contribution to the parity mixing in ^{18}F and ^{19}F.

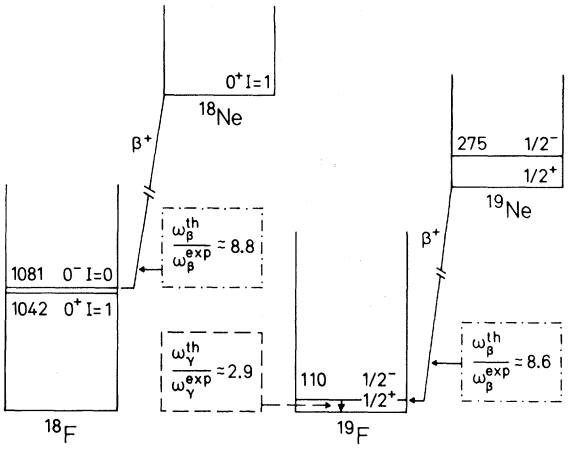

FIG. 11. β and γ analogs of the parity mixing in ^{18}F and ^{19}F. The observed suppression factors compared to predictions of the $0h\omega + 1h\omega$ shell model are shown.

(2) The $\Delta I=1$ heavy meson exchange contributions to the PNC matrix elements are negligible in all our calculations, provided the relevant couplings are within the DDH "reasonable range." Thus the experimental limit on P_γ in ^{18}F imposes a direct constraint on F_π.

(3) The *relative* strength of the $\Delta I=1$ pion and $\Delta I=0$ heavy meson PNC matrix elements in ^{19}F and ^{21}Ne is also insensitive to the nuclear model. One then expects that any scaling of calculated rates to reproduce the ^{19}F β-decay measurement is also appropriate for all the components of the PNC matrix element.

We therefore only rely on the shell model to give the relative sizes of the β decay and PNC matrix elements. We scale the absolute magnitudes of the matrix elements to reduce the measured β-decay rates in ^{18}Ne and ^{19}Ne and predict PNC matrix elements in ^{18}F and ^{19}F based on the DDH "best value" coupling constants. The nearly complete cancellation of $\Delta I=0$ and $\Delta I=1$ PNC matrix elements in ^{21}Ne makes the issue of absolute matrix elements less critical in this case (where there are no forbidden β-decay results), provided one accepts the evidence of Table VI that the relative strengths of the PNC matrix element components are unchanged by varying the model of the nuclear structure.

We conclude that the existing information on parity mixing in ^{18}F, ^{19}F, and ^{21}Ne is consistent with

weak meson-nucleon coupling constants F_π and F_0 close to the "best values" of Desplanques, Donoghue, and Holstein. This assumes that the other heavy meson couplings are not much larger than the DDH values, and that the relative scaling of matrix elements found in Table VI is general. A crucial test of our assumptions will be an investigation of the effect of $2\hbar\omega$ excitations on the β decay and PNC matrix elements in $A=19$. Will this scaling relation persist in calculations that reproduce the β-decay rate?

Our work leads to a prediction of $|P_\gamma| \sim 1.6\times10^{-3}$ for the PNC circular polarization of the 1081 keV γ ray in ^{18}F. This value was obtained by reducing the DDH values for F_π and F_0 by a factor 0.8 to reproduce the measured[7,59] A_γ for ^{19}F. As an experiment currently underway should achieve this sensitivity, the scaling relation [Eq. (23)] may soon permit a determination of F_π directly from experiment. The observation of PNC in ^{18}F will, by virtue of its pure isovector character and its connection with the ^{18}Ne β decay, provide the best constraint on hadronic weak couplings possible in complex nuclei. This constraint will simplify the interpretation of parity violating observables in ^{19}F and ^{21}Ne and will clarify important issues, such as the neutral current enhancement of F_π over the Cabibbo limit.

ACKNOWLEDGMENTS

The work was supported in part by the U.S. Department of Energy and by the National Science Foundation (Grant No. PHY8021272). One of us (E.G.A.) gratefully acknowledges financial support from the J. S. Guggenheim Foundation and the Alexander von Humboldt Stiftung which made possible enjoyable stays at Oxford and Heidelberg during which parts of this paper were written.

*Present address: Shell Oil, Western E & P, Rocky Mountain Division, P.O. Box 831, Houston, TX 77001.

†Present address: Department of Physics, Temple University, Philadelphia, PA 19122.

‡Present address: Theoretical Division, Los Alamos National Laboratory, Los Alamos, New Mexico 87545.

[1]D. E. Nagle *et al.*, in *High Energy Physics with Polarized Beams and Polarized Targets (Argonne, 1978)*, Proceedings of the Third International Symposium on High Energy Physics with Polarized Beams and Polarized Targets, AIP Conf. Proc. No. 51, edited by G. H. Thomas (AIP, New York, 1978), p. 224.

[2]R. Balzer, R. Henneck, Ch. Jacquemart, J. Lang, M. Simonius, W. Haeberli, Ch. Weddinger, W. Reichart, and S. Jaccard, Phys. Rev. Lett. 44, 699 (1980).

[3]V. M. Lobashov, private communication, states that the results given in V. M. Lobashov, D. M. Kaminker, G. I. Kharkevich, V. A. Kniazkob, N. A. Lozovoy, V. A. Nazarenko, L. F. Sayenko, L. M. Smotritsky, and A. I. Yegorov, Nucl. Phys. A197, 241 (1972), should be superceded by $|P_\gamma| < 5\times10^{-7}$.

[4]G. S. Danilov, Phys. Lett. 18, 40 (1965).

[5]J. F. Cavaignac, B. Vignon, and R. Wilson, Phys. Lett. 67B, 148 (1977).

[6]C. A. Barnes, M. M. Lowry, J. M. Davidson, R. E. Marrs, F. B. Morinigo, B. Chang, E. G. Adelberger, and H. E. Swanson, Phys. Rev. Lett. 40, 840 (1978).

[7]E. G. Adelberger, H. E. Swanson, M. D. Cooper, J. W. Tape, and T. A. Trainor, Phys. Rev. Lett. 34, 402 (1975); E. G. Adelberger, in *Polarization Phenomena in Nuclear Physics—1980 (Fifth International Symposium, Sante Fe)*, Proceedings of the Fifth International Symposium on Polarization Phenomena in Nuclear Physics, AIP Conf. Proc. No. 69, edited by G. G. Ohlsen, R. E. Brown, N. Jarmie, M. W. McNaughton, and G. M. Hale (AIP, New York, 1981), p. 1367.

[8]K. A. Snover, R. Von Lintig, E. G. Adelberger, H. E. Swanson, T. A. Trainor, A. B. McDonald, E. D. Earle, and C. A. Barnes, Phys. Rev. Lett. 41, 145 (1978); E. D. Earle, private communication.

[9]P. M. Endt and C. vanderLeun, Nucl. Phys. A310, 1 (1978); F. Ajzenberg-Selove, Nucl. Phys. A300, 1 (1978).

[10]J. Keinonen, H.-B. Mak, P. Skensved, J. R. Leslie, and W. McLatchie, Phys. Rev. C 22, 351 (1980) and J. Keinonen, H.-B. Mak, T. K. Alexander, G. C. Ball, W. G. Davies, J. S. Forester, and I. V. Mitchell, *ibid.* 23, 2073 (1981).

[11]W. N. Catford, L. K. Fifield, E. G. Garman, and D. M. Pringle, Oxford University report, 1981 (unpublished), p. 18.

[12]K. Neubeck, H. Schober, and H. Wäffler, Phys. Rev. C 10, 320 (1974).

[13]D. J. Millener, E. K. Warburton, K. A. Snover, R. Von Lintig, and P. G. Ikossi, Phys. Rev. C 18, 1878 (1978).

[14]W. C. Haxton, Phys. Rev. Lett. 46, 698 (1981); W. C. Haxton, B. F. Gibson, and E. M. Henley (unpublished).

[15]B. Desplanques, J. F. Donoghue, and B. R. Holstein, Ann. Phys. (N.Y.) 124, 449 (1980).

[16]E. K. Warburton, J. W. Olness, and C. J. Lister, Phys. Rev. C 20, 619 (1979); 23, 941(E) (1981).

[17]J. C. Hardy, H. Schmeing, J. S. Geiger, and R. L. Graham, Nucl. Phys. A223, 157 (1974).

[18]Valve numbers V52LA2026N and V52DA2100, manufactured by Skinner Electric Valves Division, New Britain, Connecticut, U.S.A.

[19]J. C. Hardy, H. Schmeing, J. S. Geiger, and R. L. Graham, Nucl. Phys. A246, 61 (1975).

[20]Pressure Transducer Type 4-424-001, manufactured by Bell and Howell, CEC Division, Pasadena, California, U.S.A.

[21]Y. Yoshizawa, Y. Iwata, T. Kaku, T. Katoh, J.-Z. Ruan, T. Kojima, and Y. Kawada, Nucl. Instrum. Methods 174, 109 (1980).

[22]E. G. Adelberger, C. D. Hoyle, H. E. Swanson, and R. D. Von Lintig, Phys. Rev. Lett. 46, 695 (1981).

[23]T. J. Bowles, private communication; A. M. Hernandez and W. W. Daehnick, Phys. Rev. C 25, 2957 (1982).

[24]C. Rolfs, H. P. Trautvetter, R. E. Azuma, and A. E. Litherland, Nucl. Phys. A199, 289 (1973).

[25]A. H. Wapstra and K. Bos, At. Data Nucl. Data Tables 19, 215 (1977).

[26]D. H. Wilkinson and B. E. F. Macefield, Nucl. Phys. A232, 58 (1974).

[27]D. E. Alburger and F. P. Calaprice, Phys. Rev. C 12, 1690 (1975).

[28]E. G. Adelberger, M. M. Hindi, C. D. Hoyle, H. E. Swanson, and R. D. Von Lintig, Phys. Rev. C 24, 313 (1981).

[29]T. W. Donnelly, D. Hitlin, M. Schwartz, J. D. Walecka, and S. J. Wiesner, Phys. Lett. 49B, 8 (1974).

[30]S. J. Freedman, R. M. Del Veccio, and C. Callias, Phys. Rev. C 12, 315 (1975).

[31]D. E. Alburger, Phys. Rev. C 13, 2593 (1976).

[32]J. D. Goss, F. L. Riffle, D. R. Parsignault, and J. C. Harris, Nucl. Phys. A115, 113 (1968).

[33]D. H. Wilkinson and D. E. Alburger, Phys. Rev. C 10, 1993 (1974).

[34]J. Jänecke, Z. Naturforsch. 15A, 593 (1960).

[35]L. G. Earwaker, J. G. Jenkin, and T. W. Titterton, Nature 195, 271 (1962).

[36]G. Azuelos and J. E. Kitching, Phys. Rev. C 12, 563 (1975).

[37]J. D. Walecka, in *Muon Physics,* edited by V. W. Hughes and C. S. Wu (Academic, New York, 1975), Vol. II.

[38]H. Behrens and J. Jänecke, *Numerical Tables for Beta-Decay and Electron Capture* (Springer, Berlin, 1969).

[39]R. P. Feynman and M. Gell-Mann, Phys. Rev. 109, 193 (1958); S. S. Gershtein and I. B. Zeldovitch, Zh. Eksp. Teor. Fiz. 29, 698 (1955) [Sov. Phys.—JETP 2, 576 (1956)].

[40]The corresponding expression in Ref. 14 contains a misprint, omission of a factor of $\frac{1}{2}$.

[41]K. Kubodera, J. Delorme, and M. Rho, Phys. Rev. Lett. 40, 755 (1978); P. A. M. Guichon, M. Giffon, and C. Samour, Phys. Lett. 74B, 15 (1978).

[42]P. G. Bizetti, T. F. Fazzini, P. R. Maurenzig, A. Perego, G. Poggi, P. Sona, and N. Taccetti, Lett. Nuovo Cimento 29, 167 (1980).

[43]G. Ahrens, W. Harfst, J. R. Kass, E. V. Mason, M. Schober, G. Steffens, H. Wäffler, P. Bock, and K. Grotz, Nucl. Phys. (to be published).

[44]W. C. Haxton, B. F. Gibson, and E. M. Henley, Phys. Rev. Lett. 45, 1677 (1980).

[45]A. B. McDonald, E. D. Earle, J. J. Simpson, R. G. H. Robertson, and H. B. Mak, Phys. Rev. Lett. 47, 1720 (1981).

[46]M. Bini, P. G. Bizzetti, and P. Sona, Phys. Rev. C 23, 1265 (1981).

[47]B. A. Brown, W. A. Richter, and N. S. Godwin, Phys. Rev. Lett. 45, 1681 (1980).

[48]T. T. S. Kuo and G. E. Brown, Nucl. Phys. A114, 241 (1968); T. T. S. Kuo, private communication.

[49]D. J. Millener and D. Kurath, Nucl. Phys. A255, 315 (1975).

[50]A. P. Zuker, Phys. Rev. Lett. 23, 983 (1969).

[51]S. Cohen and D. Kurath, Nucl. Phys. 73, 1 (1965).

[52]A. L. Fetter and J. D. Walecka, *Quantum Theory of Many-Particle Systems* (McGraw-Hill, New York, 1971).

[53]I. S. Towner and F. C. Khanna, Nucl. Phys. A372, 331 (1981); I. S. Towner, in Proceedings of the International Conference on Spin Excitations in Nuclei, Telluride, Colorado, 1982 (to be published).

[54]M. A. Box, B. H. J. McKellar, P. Pick, and K. R. Lassey, J. Phys. G 1, 493 (1975); F. C. Michel, Phys. Rev. 133, B329 (1964); J. B. Adams, *ibid.* 156, 1611 (1967); B. D. Serot, Nucl. Phys. A322, 408 (1979).

[55]G. A. Miller and J. E. Spencer, Ann. Phys. (N.Y.) 100, 562 (1976).

[56]H.-B. Mak, private communication.

[57]K. Koshigiri, H. Ohtsubo, and M. Morita, Prog. Theor. Phys. 62, 706 (1979); P. A. M. Guichon and C. Samour, Lyon Report No. DPhN-HE/81-9 (unpublished).

[58]S. Nozawa, Y. Kohyama, and K. Kubodera, Prog. Theor. Phys. 67, 1240 (1982).

[59]K. Elsener, W. Grüebler, V. König, C. Schweizer, P. A. Schmelzbach, J. Ulbricht, F. Sperisen, and M. Merdzan, Phys. Lett. 117B, 167 (1982).